



Article

Event-Triggered Adaptive Neural Network Control for State-Constrained Pure-Feedback Fractional-Order Nonlinear Systems with Input Delay and Saturation

Changhui Wang * , Jiaqi Yang and Mei Liang *

School of Electromechanical and Automotive Engineering, Yantai University, 32 Qingquan Road, Yantai 264005, China; jiaqiyang@126.com

* Correspondence: wang_changhui@126.com (C.W.); mmglm@163.com (M.L.)

Abstract: In this research, the adaptive event-triggered neural network controller design problem is investigated for a class of state-constrained pure-feedback fractional-order nonlinear systems (FONSs) with external disturbances, unknown actuator saturation, and input delay. An auxiliary compensation function based on the integral function of the input signal is presented to handle input delay. The barrier Lyapunov function (BLF) is utilized to deal with state constraints, and the event-triggered strategy is applied to overcome the communication burden from the limited communication resources. By the utilization of a backstepping scheme and radial basis function neural network, an adaptive event-triggered neural state-feedback stabilization controller is constructed, in which the fractional-order dynamic surface filters are employed to reduce the computational burden from the recursive procedure. It is proven that with the fractional-order Lyapunov analysis, all the solutions of the closed-loop system are bounded, and the tracking error can converge to a small interval around the zero, while the state constraint is satisfied and the Zeno behavior can be strictly ruled out. Two examples are finally given to show the effectiveness of the proposed control strategy.

Keywords: nonlinear system; event-triggered control; BLF; constraints; input delay



Citation: Wang, C.; Yang, J.; Liang, M. Event-Triggered Adaptive Neural Network Control for State-Constrained Pure-Feedback Fractional-Order Nonlinear Systems with Input Delay and Saturation. *Fractal Fract.* **2024**, *8*, 256. <https://doi.org/10.3390/fractalfract8050256>

Academic Editors: Xujun Yang and Xiaofeng Chen

Received: 8 March 2024

Revised: 12 April 2024

Accepted: 18 April 2024

Published: 26 April 2024



Copyright: © 2024 by the authors. Licensee MDPI, Basel, Switzerland. This article is an open access article distributed under the terms and conditions of the Creative Commons Attribution (CC BY) license (<https://creativecommons.org/licenses/by/4.0/>).

1. Introduction

Fractional-order dynamical behavior has been found in many practical systems [1,2], which can achieve more precise representations for complex physical systems with infinite memory and genetic characteristics. Based on this fact, fractional-order nonlinear systems (FONSs) offer an effective way to model the physical system [3,4], which can be applied in lots of areas [5–9]. Moreover, the nonlinear controller design problem for FONSs has received a lot of attention, and many controller design approaches have been investigated [10–15], in which the approximation performance of fuzzy logic systems (FLSs) or neural networks (NNs) can be used to deal with nonlinear unknown function in FONSs to achieve stability. In [16], an adaptive controller by using the property of NNs is considered for FONSs with actuator fault. In [17], a fuzzy controller is designed for nonstrict-feedback FONSs. In [18], a distributed backstepping control for nonaffine FONSs with unknown dynamics is presented, and the stability is accomplished. For fractional-order tumor systems with chemotherapy in [19], a finite-time fuzzy controller is developed under Lyapunov theory. It is worth noting that the influence of full state constraints on FONSs has not been taken into account in the above-mentioned literature and achievements.

System constraints often appear in many real industrial processes and practical systems unavoidably, which is the main factor limiting system performance, leading to instability of the system. To settle such system constraints, a crucial problem for FONSs, the barrier Lyapunov function (BLF) has become one of the most powerful tools to prevent transgression of state constraints, and many constraint control strategies have been designed [20–23]. In [21], an observer-based adaptive NN controller is proposed for nonstrict-feedback FONSs with

an output constraint, where the tracking error satisfying constraints can be guaranteed. In [22], a distributed adaptive controller is designed for multiple FONSs with constraints, and the BLF is applied to restrict the output in the preset range. In [23], an adaptive dynamic surface controller for FONSs with asymmetric state constraints is designed by using an asymmetric BLF. Nevertheless, it is important that the characteristics of the control input signal should not be ignored.

It is inevitable that the input saturation is the important non-smooth nonlinearity in many practical engineering systems due to the physical characteristics of the actuator. Once the control input exceeds the upper, it may not work properly and can unquestionably limit its control performance. Then, it is important to take the effect of actuator saturation into consideration during the process of the design and analysis of FONSs [24–26]. The author in [24] introduced the fractional-order finite-time adaptive fault-tolerant control for an unmanned aerial vehicle with the saturated actuator, wherein the input saturation function is approximated using the smooth function. In [26], the flexible spacecraft attitude adjustment with input torque saturation is considered, and a fractional-order multi-objective controller is presented. For a vertical takeoff vertical landing reusable launch vehicle subjected to input saturation constraints, a fractional-order fixed-time sliding mode controller with state observer is designed in [25]. However, in the above-mentioned research for FONSs, the issue of the widely existing input delay is ignored.

In the control process for real engineering applications, it takes time to send signals to actuators causing the input delays of the system, and is the major factor in deteriorating the system performance. To deal with the input delay, many effective methods are developed for FONSs in [27–30]. In [27], a feedback controller for a fractional-order system under input delay is designed by using the Smith predictor. In [28], an augmented adaptive controller based on the function approximation technique is developed for FONSs with input delay. In [29], a command-filter-based adaptive controller for FONSs with input delay is designed by using the fractional integral. In [30], an adaptive NN control method for FONSs with input delay is developed by using the auxiliary system. However, no results about the adaptive control strategy of state-constrained FONSs with input delay and actuator saturation can be found.

Motivated by the above-mentioned discussions, the adaptive neural network event-triggered control (ETC) for state-constrained pure-feedback FONSs with input delay and unknown actuator saturation will be investigated. The highlighted innovations of this article are as follows:

- (1) Compared with fractional-order controller results [31–33], the full-state constraints, input delay, and unknown actuator saturation are investigated simultaneously in this article, and the BLFs and neural network are introduced into the design process of the backstepping technique, which can ensure that state convergence without contravening state constraints can be guaranteed, and the boundedness of all the closed-loop system signals can be accomplished.
- (2) Compared with controller designed for FONSs subject to input delay in [27–30,34], the event-triggered mechanism is designed to reduce the communications constraints of network resources, and the fractional-order dynamic surface filter is presented to remove the explosion of differentiation from the recursive procedure, which effectively makes the proposed controller more suitable for practical engineering.

The rest of this paper is organized as follows. The preliminaries and problem formulation are presented in Sections 2 and 3, respectively. Then, the proposed adaptive control scheme for FONSs with input delay is provided in Section 4. The simulation studies are given in Section 5 to show the effectiveness. Section 6 concludes this paper.

2. Preliminaries

The α th Caputo fractional derivative of $f(t)$ is defined as [35,36]:

$$D_{t_0}^\alpha f(t) = \frac{1}{\Gamma(n-\alpha)} \int_{t_0}^t \frac{f^{(n)}(\tau)}{(t-\tau)^{\alpha+1-n}} d\tau$$

where $n-1 < \alpha < n$, n is the positive integer, $\Gamma(\alpha) = \int_0^\infty e^{-t} t^{\alpha-1} dt$ is the Euler Gamma function, and $D_{t_0}^\alpha$ can be abbreviated as D^α , when $t_0 = 0$.

Lemma 1 ([35]). If $\phi \in (\frac{\pi\alpha}{2}, \pi\alpha)$, then $\exists \beta > 0$, such that

$$|E_{\alpha,\gamma}(\zeta)| \leq \frac{\beta}{1+|\zeta|}, \gamma \leq |\arg(\zeta)| \leq \pi, |\zeta| \geq 0$$

where $E_{\alpha,\gamma}(\zeta) = \sum_{k=0}^{\infty} \frac{\zeta^k}{\Gamma(\alpha k + \gamma)}$ is the one-parameter Mittag-Leffler function, ζ is a complex number, and $\alpha, \gamma > 0$. Note that $E_{\alpha,1}(\zeta) = E_\alpha(\zeta)$ and $E_{1,1}(\zeta) = e^\zeta$.

Lemma 2 ([37,38]). Let $x(t) \in \mathbb{R}^n$ be a differentiable function. Then, $D^\alpha(x^T(t)Px(t)) \leq 2x^T(t)PD^\alpha(x(t))$ holds for $\forall t \geq t_0$, where $P = P^T > 0$.

Lemma 3 ([39]). Let $h_1(\cdot), h_2(\cdot) \in \mathbb{R}$ be smooth functions. If $h_1(h_2)$ is convex (i.e., $\partial^2 h_1(h_2)/\partial h_2^2 \geq 0$), then, $D^\alpha h_1(h_2) \leq \partial h_1(h_2)/\partial h_2 \cdot D^\alpha h_2$ for $\forall t \geq 0$.

Lemma 4 ([40]). Let the function $V(t) : \mathbb{R}^+ \rightarrow \mathbb{R}$ satisfying $D^\alpha V(t) + \eta V(t) \leq \mu$, where $\eta > 0$, and $\mu \geq 0$. Then, $V(t) \leq V(0)E_{(\alpha,1)}(-\eta t^\alpha) + \frac{\mu^\vartheta}{\eta}$, where $\vartheta = \max\{1, \beta\}$ and β is defined in Lemma 1.

Lemma 5 ([41,42]). For $\forall k_{b_0} > 0$, the following inequality holds

$$\ln \frac{k_{b_0}^2}{k_{b_0}^2 - \zeta^2(t)} \leq \frac{\zeta^2(t)}{k_{b_0}^2 - \zeta^2(t)}$$

if $|\zeta(t)| \leq k_{b_0}$.

Lemma 6 ([43]). For $\forall \varepsilon^* > 0$ and $s \in \mathbb{R}$, it holds $|s| - s \tanh(\frac{s}{\varepsilon^*}) \leq 0.2785\varepsilon^*$.

Lemma 7 ([44]). Let $h(x)$ be a continuous function. For $\forall \varepsilon > 0$, there is a radial basis function NN (RBFNN) $W^T \Psi(x)$ satisfying $h(x) = W^T \Psi(x) + \varepsilon$, where $W = (w_1 \ w_2 \ \dots \ w_N)^T$, ε is an approximation error. $\Psi(x) = (\psi_1(x) \ \psi_2(x) \ \dots \ \psi_N(x))^T / \sum_{i=1}^N \psi_i(x) \in \mathbb{R}^N$, $N > 1$ denotes node number, $\psi_i(x) = \exp\left(-\frac{(x-l_i)^T(x-l_i)}{\chi_i^T \chi_i}\right)$, $l_i = (l_{i1} \ l_{i2} \ \dots \ l_{in})^T$, and $\chi_i = (\chi_{i1} \ \chi_{i2} \ \dots \ \chi_{in})^T$.

3. System Descriptions and Problem Formulation

A class of pure-feedback FONSs with input delay and unknown actuator saturation is considered as follows:

$$\begin{cases} D^\alpha x_i = f_i(\bar{x}_i, x_{i+1}) + d_i(t), i = 1, 2, \dots, n-1 \\ D^\alpha x_n = f_n(\bar{x}_n) + u(v(t-\tau)) + d_n(t) \\ y = x_1 \end{cases} \quad (1)$$

where $\alpha \in (0, 1]$, $\bar{x}_i = (x_1 \ x_2 \ \dots \ x_i)^T \in \mathbb{R}^i$ denotes the system state, $y \in \mathbb{R}$ denotes the output, $f_i(\cdot)$ denotes an unknown smooth function, and $d_i(t)$ denotes bounded distur-

bance, $i = 1, 2, \dots, n$. $\tau \in \mathbb{R}^+$ represents input delay, v denotes the controller input to be designed, and $u(v)$ denotes the systems input with saturation defined as:

$$u(v) = \begin{cases} u_{\max}, & v \geq u_{\max} \\ v, & u_{\min} < v < u_{\max} \\ u_{\min}, & v \leq u_{\min} \end{cases} \quad (2)$$

where $u_{\max} > 0$ and $u_{\min} < 0$ are unknown constants. Saturation (2) can be denoted as [45,46]:

$$u(v) = h(v) + \Delta(v)$$

where $\Delta(v) = u(v) - h(v)$, $|\Delta(v)| \leq \max\{u_{\max}(1 - \tanh(1)), u_{\min}(\tanh(1) - 1)\} = \bar{D}$, and

$$h(v) = \begin{cases} u_{\max} \cdot \frac{e^{\frac{v}{u_{\max}}} - e^{-\frac{v}{u_{\max}}}}{e^{\frac{v}{u_{\max}}} + e^{-\frac{v}{u_{\max}}}}, & v \geq 0 \\ u_{\min} \cdot \frac{e^{\frac{v}{u_{\min}}} - e^{-\frac{v}{u_{\min}}}}{e^{\frac{v}{u_{\min}}} + e^{-\frac{v}{u_{\min}}}}, & v < 0 \end{cases}$$

There is a constant $\mu, 0 < \mu < 1$, and we obtain $h(v) = h_{v_\mu}v$ when selecting $v_0 = 0$, and

$$u(v) = h_{v_\mu}v + \Delta(v)$$

where $0 < h_{\min} \leq |h_{v_\mu}| \leq 1$, h_{\min} is an unknown constant. Without loss of generality, it is assumed that $h_{v_\mu} > 0$.

In fact, many physical systems can be modeled by pure-feedback FONSs with input delay and actuator saturation, such as rotational mechanical system [47], power systems [48], single-machine-infinite bus system [49], and Chua–Hartley’s system [50].

The control goal is to develop an adaptive event-triggered neural network controller for (2) s.t.: (1) y can track the desired $y_r(t)$; (2) All the states are constrained in a compact set, i.e., $x_i \in \{x_i | |x_i| < k_{c_i}, k_{c_i} > 0\}$.

Since $f_i(\bar{x}_i, x_{i+1})$ is an unknown smooth function, the partial derivative $g_i(\bar{x}_i, x_{i+1}) = \partial f_i(\bar{x}_i, x_{i+1}) / \partial x_{i+1}$ is continuous, $i = 1, 2, \dots, n - 1$. According to the mean-value theorem [51], $\exists \eta_i \in (0, 1)$, such that

$$f_i(\bar{x}_i, x_{i+1}) = f_i(\bar{x}_i, 0) + g_i(\bar{x}_i, \eta_i x_{i+1})x_{i+1} \quad i = 1, 2, \dots, n - 1 \quad (3)$$

Assumption 1. There are unknown constants $0 < g_{i \min} \leq g_{i \max} < \infty$, s.t. $0 < g_{i \min} \leq |g_i(\bar{x}_i, \eta_i x_{i+1})| \leq g_{i \max}$, $i = 1, 2, \dots, n - 1$. Without loss of generality, it is assumed that $0 < g_{i \min} \leq g_i(\bar{x}_i, \eta_i x_{i+1}) \leq g_{i \max}$, $i = 1, 2, \dots, n - 1$.

Assumption 2. The disturbance $d_i(t)$ is bounded, and satisfies $|d_i(t)| \leq \bar{d}_i$ with $\bar{d}_i > 0$.

Assumption 3. For $\forall k_{c_1} > 0$, there are positive constants A_0, A_1 , and A_2 , such that $|y_r| \leq A_0 < k_{c_1}$, $|D^\alpha y_r(t)| \leq A_1$, and $|D^{2\alpha} y_r(t)| \leq A_2$. There is a compact $\Omega_{y_r} = \left\{ (y_r \ D^\alpha y_r \ D^{2\alpha} y_r)^T \mid y_r^2 + (D^\alpha y_r)^2 + (D^{2\alpha} y_r)^2 \leq \delta_{y_r}, \delta_{y_r} > 0 \right\}$, s.t. $(y_r \ D^\alpha y_r \ D^{2\alpha} y_r)^T \in \Omega_{y_r}$.

4. Control Scheme Design and Stability Analysis

4.1. Control Design

In this section, the adaptive neural network control method will be given for the systems (2) by combining the backstepping technology with a fractional-order dynamic surface filter, and the block diagram is shown in Figure 1. The detailed design process will be given in the following steps.

First, define the coordinate transformations as:

$$\chi_1 = y - y_r, \chi_i = x_i - a_{i,l}, \chi_n = x_n - a_{n,l} + u_s(t), i = 2, 3, \dots, n - 1 \tag{4}$$

where $u_s(t)$ is the fractional-order differential and integral signal defined as

$$u_s(t) = D^{1-\alpha} \int_{t-\tau}^t u(v(z)) dz \tag{5}$$

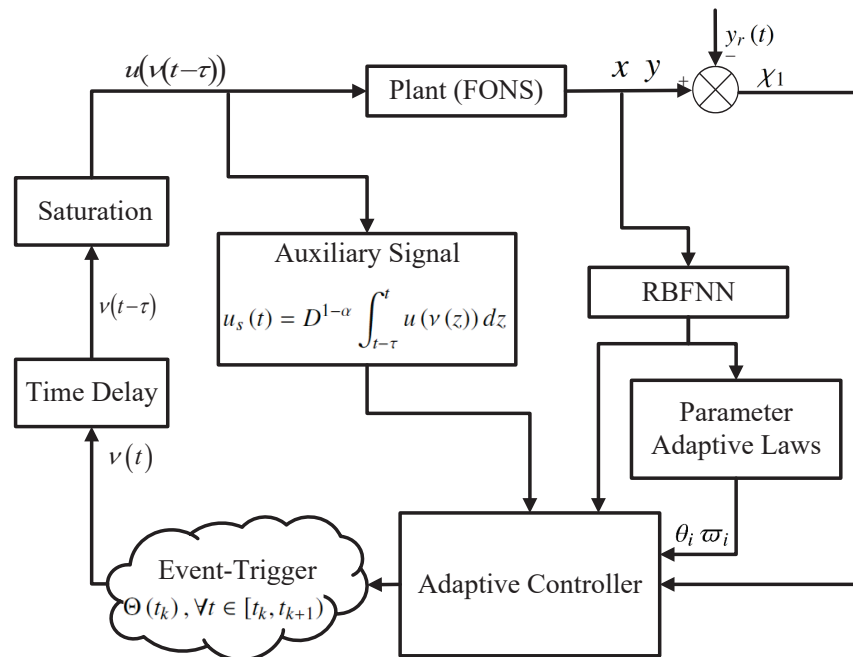


Figure 1. The block diagram of the proposed controller.

The above auxiliary signal $u_s(t)$ is employed to handle the input delay, and it is natural to assume that $u_s(t)$ bounded by $|u_s(t)| \leq \bar{u}_s, \bar{u}_s > 0$ is an unknown constant.

The fractional-order dynamic surface filter is designed as

$$\kappa_i D^\alpha a_{i,l} = -a_{i,l} + a_{i-1}, a_{i,l}(0) = a_{i-1}(0). \tag{6}$$

where a_{i-1} is the virtual controller, and κ_i is a constant. Define filter output error as $\zeta_i = a_{i,l} - a_{i-1}, i = 2, 3, \dots, n$.

Step 1: From (1), (3), and (4), the Caputo fractional derivative of χ_1 can be presented as

$$\begin{aligned} D^\alpha \chi_1 &= f_1(\bar{x}_1, x_2) + d_1(t) - D^\alpha y_r(t) \\ &= f_1(\bar{x}_1, 0) + g_1(\bar{x}_1, \eta_1 x_2)(\chi_2 + \zeta_2 + a_1) + d_1(t) - D^\alpha y_r(t) \end{aligned}$$

where the function $F(X_1) = f_1(\bar{x}_1, 0) + g_1(\bar{x}_1, \eta_1 x_2)\chi_2 - D^\alpha y_r(t)$ is unknown, $X_1 = (\bar{x}_2, y_r)$. The RBFNN $W_{X_1}^{*T} \Psi_{X_1}(X_1)$ is utilized to approximate $F(X_1)$ by using Lemma 7, and $W_{X_1}^*$ is the optimal parameter vector. Then, for $\forall \bar{\epsilon}_1 > 0$, it holds $F_1(X_1) = W_{X_1}^{*T} \Psi_{X_1}(X_1) + \epsilon_1(X_1), |\epsilon_1(X_1)| < \bar{\epsilon}_1$. Then, one can obtain

$$\begin{aligned} D^\alpha \chi_1 &= W_{X_1}^{*T} \Psi_{X_1}(X_1) + \epsilon_1(X_1) \\ &\quad + g_1(\bar{x}_1, \eta_1 x_2)(\zeta_2 + a_1) + d_1(t) \end{aligned} \tag{7}$$

The candidate function is chosen as $V_1 = \frac{1}{2} \ln \frac{k_{b_1}^2}{k_{b_1}^2 - \chi_1^2} + \frac{\delta_{1 \min}}{2\gamma_1} \tilde{\theta}_1^2 + \frac{\delta_{1 \min}}{2\zeta_1} \tilde{\omega}_1^2$, where $k_{b_1} = k_{c_1} - A_0$. $\gamma_1 > 0$ and $\zeta_1 > 0$ are the design parameters. $\tilde{\theta}_1 = \theta_1^* - \theta_1$ is the parameter

estimation error with the estimate θ_1 of the parameter $\theta_1^* = \|W_{X_1}^*\|^2 / g_{1 \min} \cdot \tilde{\omega}_1 = \omega_1^* - \omega_1$ is estimation error with the upper bound $\omega_1^* = \bar{\varepsilon}_1^2 + \bar{d}_1^2$, and ω_1 is the parameter estimation of ω_1^* . According to (7), Assumption 1, Lemma 2, and Lemma 3, we obtain

$$\begin{aligned} D^\alpha V_1 &= \frac{\chi_1}{k_{b_1}^2 - \chi_1^2} D^\alpha \chi_1 - \frac{g_{1 \min}}{\gamma_1} \tilde{\theta}_1 D^\alpha \theta_1 - \frac{g_{1 \min}}{\varsigma_1} \tilde{\omega}_1 D^\alpha \omega_1 \\ &= \frac{\chi_1}{k_{b_1}^2 - \chi_1^2} \left(W_{X_1}^{*\Gamma} \Psi_{X_1}(X_1) + \varepsilon_1(X_1) + g_1(\bar{x}_1, \eta_1 x_2) (\zeta_2 + a_1) \right) \\ &\quad + \frac{\chi_1}{k_{b_1}^2 - \chi_1^2} d_1(t) - \frac{g_{1 \min}}{\gamma_1} \tilde{\theta}_1 D^\alpha \theta_1 - \frac{g_{1 \min}}{\varsigma_1} \tilde{\omega}_1 D^\alpha \omega_1 \end{aligned} \tag{8}$$

The Young’s inequality is used, and we obtain:

$$\frac{\chi_1}{k_{b_1}^2 - \chi_1^2} W_{X_1}^{*\Gamma} \Psi_{X_1}(X_1) \leq \frac{g_{1 \min} \chi_1^2}{2c_1^2 (k_{b_1}^2 - \chi_1^2)^2} \theta_1^* \|\Psi_{X_1}(X_1)\|^2 + \frac{c_1^2}{2} \tag{9}$$

$$\frac{\chi_1}{k_{b_1}^2 - \chi_1^2} \varepsilon_1(X_1) \leq \frac{g_{1 \min} \bar{\varepsilon}_1^2 \chi_1^2}{2\bar{\zeta}_1^2 (k_{b_1}^2 - \chi_1^2)^2} + \frac{\bar{\zeta}_1^2}{2g_{1 \min}} \tag{10}$$

$$\frac{\chi_1}{k_{b_1}^2 - \chi_1^2} g_1(\bar{x}_1, \eta_1 x_2) \zeta_2 \leq \frac{g_{1 \min} \chi_1^2}{2\delta_1^2 (k_{b_1}^2 - \chi_1^2)^2} + \frac{\delta_1^2 g_{1 \max}^2 \zeta_2^2}{2g_{1 \min}} \tag{11}$$

$$\frac{\chi_1}{k_{b_1}^2 - \chi_1^2} d_1(t) \leq \frac{g_{1 \min} \bar{d}_1^2 \chi_1^2}{2\bar{\zeta}_1^2 (k_{b_1}^2 - \chi_1^2)^2} + \frac{\bar{\zeta}_1^2}{2g_{1 \min}} \tag{12}$$

where $c_1, \bar{\zeta}_1, \delta_1 > 0$.

Substituting (9)–(12) into (8) with Assumption 1 yields

$$\begin{aligned} D^\alpha V_1 &\leq \frac{\chi_1}{k_{b_1}^2 - \chi_1^2} g_1(\bar{x}_1, \eta_1 x_2) a_1 + \frac{g_{1 \min} \chi_1^2}{2c_1^2 (k_{b_1}^2 - \chi_1^2)^2} \theta_1^* \|\Psi_{X_1}(X_1)\|^2 \\ &\quad + \frac{g_{1 \min} \omega_1^* \chi_1^2}{2\bar{\zeta}_1^2 (k_{b_1}^2 - \chi_1^2)^2} + \frac{\bar{\zeta}_1^2}{g_{1 \min}} + \frac{g_{1 \min} \chi_1^2}{2\delta_1^2 (k_{b_1}^2 - \chi_1^2)^2} + \frac{\delta_1^2 g_{1 \max}^2 \zeta_2^2}{2g_{1 \min}} \\ &\quad - \frac{g_{1 \min}}{\gamma_1} \tilde{\theta}_1 D^\alpha \theta_1 - \frac{g_{1 \min}}{\varsigma_1} \tilde{\omega}_1 D^\alpha \omega_1 + \frac{c_1^2}{2} \\ &\leq \frac{\chi_1}{k_{b_1}^2 - \chi_1^2} \left(g_1(\bar{x}_1, \eta_1 x_2) a_1 + \frac{g_{1 \min} \chi_1}{2c_1^2 (k_{b_1}^2 - \chi_1^2)^2} \theta_1 \|\Psi_{X_1}(X_1)\|^2 \right) \\ &\quad + \frac{\chi_1}{k_{b_1}^2 - \chi_1^2} \left(\frac{g_{1 \min} \chi_1}{2\bar{\zeta}_1^2 (k_{b_1}^2 - \chi_1^2)^2} \omega_1 + \frac{g_{1 \min} \chi_1}{2\delta_1^2 (k_{b_1}^2 - \chi_1^2)^2} \right) \\ &\quad + \frac{c_1^2}{2} + \frac{\bar{\zeta}_1^2}{g_{1 \min}} + \frac{\delta_1^2 g_{1 \max}^2 \zeta_2^2}{2g_{1 \min}} \\ &\quad - g_{1 \min} \tilde{\theta}_1 \left(\frac{1}{\gamma_1} D^\alpha \theta_1 - \frac{\chi_1^2}{2c_1^2 (k_{b_1}^2 - \chi_1^2)^2} \|\Psi_{X_1}(X_1)\|^2 \right) \\ &\quad - g_{1 \min} \tilde{\omega}_1 \left(\frac{1}{\varsigma_1} D^\alpha \omega_1 - \frac{\chi_1^2}{2\bar{\zeta}_1^2 (k_{b_1}^2 - \chi_1^2)^2} \right) \end{aligned} \tag{13}$$

The virtual controller and adaptive laws are designed as

$$a_1 = -b_1\chi_1 - \frac{\chi_1}{2c_1^2(k_{b_1}^2 - \chi_1^2)}\theta_1 \|\Psi_{X_1}(X_1)\|^2 - \frac{\chi_1}{2\zeta_1^2(k_{b_1}^2 - \chi_1^2)}\omega_1 - \frac{\chi_1}{2\delta_1^2(k_{b_1}^2 - \chi_1^2)} \quad (14)$$

$$D^\alpha \theta_1 = \frac{\gamma_1 \chi_1^2}{2c_1^2(k_{b_1}^2 - \chi_1^2)^2} \|\Psi_{X_1}(X_1)\|^2 - \phi_1 \theta_1 \quad (15)$$

$$D^\alpha \omega_1 = \frac{\varsigma_1 \chi_1^2}{2\zeta_1^2(k_{b_1}^2 - \chi_1^2)^2} - \varphi_1 \omega_1 \quad (16)$$

where $b_1 > 0, \gamma_1 > 0, \varsigma_1 > 0, \phi_1 > 0$ and $\varphi_1 > 0$.

Substituting (14)–(16) into (13), $D^\alpha V_1$ is represented as:

$$D^\alpha V_1 \leq -\frac{b_1 g_1 \min \chi_1^2}{k_{b_1}^2 - \chi_1^2} + \frac{c_1^2}{2} + \frac{\zeta_1^2}{g_1 \min} + \frac{\delta_1^2 g_1^2 \max}{2g_1 \min} \zeta_2^2 + \frac{1}{\gamma_1} g_1 \min \phi_1 \tilde{\theta}_1 \theta_1 + \frac{1}{\varsigma_1} g_1 \min \varphi_1 \tilde{\omega}_1 \omega_1 \quad (17)$$

Step i ($i = 2, 3, \dots, n - 2$): Taking the Caputo fractional derivative of χ_i yields

$$D^\alpha \chi_i = f_i(\bar{x}_i, 0) + d_i(t) - D^\alpha a_{i,l} + g_i(\bar{x}_i, \eta_i x_{i+1})(\chi_{i+1} + \zeta_{i+1} + a_i)$$

Using Lemma 7, the unknown nonlinear function $F_i(X_i) = f_i(\bar{x}_i, 0) + g_i(\bar{x}_i, \eta_i x_{i+1})\chi_{i+1} - D^\alpha a_{i,l}$ is approximated by RBFNN $W_{X_i}^{*\top} \Psi_{X_i}(X_i)$, and $W_{X_i}^*$ is the optimal parameter vector. Then, $F_i(X_i) = W_{X_i}^{*\top} \Psi_{X_i}(X_i) + \varepsilon_i(X_i)$, $|\varepsilon_i(X_i)| < \bar{\varepsilon}_i$, where $\bar{\varepsilon}_i > 0$, and one can obtain

$$D^\alpha \chi_i = W_{X_i}^{*\top} \Psi_{X_i}(X_i) + \varepsilon_i(X_i) + g_i(\bar{x}_i, \eta_i x_{i+1})(\zeta_{i+1} + a_i) + d_i(t) \quad (18)$$

Select the Lyapunov function candidate $V_i = V_{i-1} + \frac{1}{2} \ln \frac{k_{b_i}^2}{k_{b_i}^2 - \chi_i^2} + \frac{g_i \min}{2\gamma_i} \tilde{\theta}_i^2 + \frac{g_i \min}{2\varsigma_i} \tilde{\omega}_i^2 + \frac{1}{2} \zeta_i^2$, where $k_{b_i} > 0$ and its definition will be obtained later. $\gamma_i > 0$ and $\varsigma_i > 0$ are the design parameters. $\tilde{\theta}_i = \theta_i^* - \theta_i$ is the parameter estimation error with the estimate θ_i of the parameter $\theta_i^* = \frac{\|W_{X_i}^*\|^2}{g_i \min}$. $\tilde{\omega}_i = \omega_i^* - \omega_i$ is the parameter estimation error with the upper bound $\omega_i^* = \bar{\varepsilon}_i^2 + \bar{d}_i^2$, and ω_i is the parameter estimation of ω_i^* .

Similar to the analysis in Step 1 using Young's inequality yields:

$$\frac{\chi_i}{k_{b_i}^2 - \chi_i^2} W_{X_i}^{*\top} \Psi_{X_i}(X_i) \leq \frac{g_i \min \chi_i^2}{2c_i^2(k_{b_i}^2 - \chi_i^2)^2} \theta_i^* \|\Psi_{X_i}(X_i)\|^2 + \frac{c_i^2}{2} \quad (19)$$

$$\frac{\chi_i}{k_{b_i}^2 - \chi_i^2} \varepsilon_i(X_i) \leq \frac{g_i \min \bar{\varepsilon}_i^2 \chi_i^2}{2\zeta_i^2(k_{b_i}^2 - \chi_i^2)^2} + \frac{\zeta_i^2}{2g_i \min} \quad (20)$$

$$\frac{\chi_i}{k_{b_i}^2 - \chi_i^2} g_i(\bar{x}_i, \eta_i x_{i+1}) \zeta_{i+1} \leq \frac{g_i \min \chi_i^2}{2\delta_i^2(k_{b_i}^2 - \chi_i^2)^2} + \frac{\delta_i^2 g_i^2 \max}{2g_i \min} \zeta_{i+1}^2 \quad (21)$$

$$\frac{\chi_i}{k_{b_i}^2 - \chi_i^2} d_i(t) \leq \frac{g_i \min d_i^2 \chi_i^2}{2\bar{c}_i^2 (k_{b_i}^2 - \chi_i^2)^2} + \frac{\bar{\zeta}_i^2}{2g_i \min} \tag{22}$$

where $c_i, \bar{\zeta}_i, \delta_i > 0$.

From (19) to (22) with Assumption 1, one can obtain

$$\begin{aligned} D^\alpha V_i &\leq D^\alpha V_{i-1} + \frac{\chi_i}{k_{b_i}^2 - \chi_i^2} g_i(\bar{x}_i, \eta_i x_{i+1}) a_i \\ &+ \frac{g_i \min \chi_i^2}{2c_i^2 (k_{b_i}^2 - \chi_i^2)^2} \theta_i^* \|\Psi_{X_i}(X_i)\|^2 + \frac{g_i \min \omega_i^* \chi_i^2}{2\bar{c}_i^2 (k_{b_i}^2 - \chi_i^2)^2} \\ &+ \frac{g_i \min \chi_i^2}{2\delta_i^2 (k_{b_i}^2 - \chi_i^2)^2} + \frac{c_i^2}{2} + \frac{\bar{\zeta}_i^2}{g_i \min} + \frac{\delta_i^2 g_i \max \zeta_{i+1}^2}{2g_i \min} \\ &- \frac{g_i \min}{\gamma_i} \bar{\theta}_i D^\alpha \theta_i - \frac{g_i \min}{\zeta_i} \bar{\omega}_i D^\alpha \omega_i + \zeta_i D^\alpha \zeta_i \end{aligned} \tag{23}$$

Design virtual controller a_i and adaptive laws as

$$\begin{aligned} a_i &= -b_i \chi_i - \frac{\chi_i}{2c_i^2 (k_{b_i}^2 - \chi_i^2)} \|\Psi_{X_i}(X_i)\|^2 \theta_i \\ &- \frac{\chi_i}{2\bar{c}_i^2 (k_{b_i}^2 - \chi_i^2)} \omega_i - \frac{\chi_i}{2\delta_i^2 (k_{b_i}^2 - \chi_i^2)} \end{aligned} \tag{24}$$

$$D^\alpha \theta_i = \frac{\gamma_i \chi_i^2}{2c_i^2 (k_{b_i}^2 - \chi_i^2)^2} \|\Psi_{X_i}(X_i)\|^2 - \phi_i \theta_i \tag{25}$$

$$D^\alpha \omega_i = \frac{\zeta_i \chi_i^2}{2\bar{c}_i^2 (k_{b_i}^2 - \chi_i^2)^2} - \phi_i \omega_i \tag{26}$$

where $b_i > 0, \gamma_i > 0, \zeta_i > 0, \phi_i > 0$, and $\phi_i > 0$ are the tunable parameters.

Based on (24)–(26), (23) is described as

$$\begin{aligned} D^\alpha V_i &\leq D^\alpha V_{i-1} - \frac{g_i \min b_i \chi_i^2}{k_{b_i}^2 - \chi_i^2} + \frac{c_i^2}{2} + \frac{\bar{\zeta}_i^2}{g_i \min} + \frac{\delta_i^2 g_i \max \zeta_{i+1}^2}{2g_i \min} \\ &+ \frac{g_i \min}{\gamma_i} \phi_i \bar{\theta}_i \theta_i - \frac{g_i \min}{\zeta_i} \phi_i \bar{\omega}_i \omega_i + \zeta_i D^\alpha \zeta_i \\ &\leq - \sum_{i=1}^{n-1} \frac{b_i g_i \min \chi_i^2}{k_{b_i}^2 - \chi_i^2} + \sum_{i=1}^{n-1} \frac{\bar{\zeta}_i^2}{g_i \min} + \sum_{i=1}^{n-1} \frac{c_i^2}{2} + \sum_{i=1}^{n-1} \frac{\delta_i^2 g_i \max \zeta_{i+1}^2}{2g_i \min} \\ &+ \sum_{i=1}^{n-1} \frac{g_i \min}{\gamma_i} \phi_i \bar{\theta}_i \theta_i + \sum_{i=1}^{n-1} \frac{g_i \min}{\zeta_i} \phi_i \bar{\omega}_i \omega_i + \sum_{i=2}^{n-1} \zeta_i D^\alpha \zeta_i \end{aligned} \tag{27}$$

Step $i = n - 1$: Taking the Caputo fractional derivative of χ_{n-1} yields

$$\begin{aligned} D^\alpha \chi_{n-1} &= f_{n-1}(\bar{x}_{n-1}, 0) + d_{n-1}(t) - D^\alpha a_{n-1} \\ &+ g_{n-1}(\bar{x}_{n-1}, \eta_{n-1} x_n)(\chi_n + \zeta_n + a_{n-1} - u_s(t)) \end{aligned}$$

Using Lemma 7, the unknown nonlinear function $F_{n-1}(X_{n-1}) = f_{n-1}(\bar{x}_{n-1}, 0) + g_{n-1}(\bar{x}_{n-1}, \eta_{n-1} x_n)\chi_n - D^\alpha a_{n-1}$ is approximated by RBFNN $W_{X_{n-1}}^{*\text{T}} \Psi_{X_{n-1}}(X_{n-1})$, and $W_{X_{n-1}}^*$ is the optimal parameter vector, then $F_{n-1}(X_{n-1}) = W_{X_{n-1}}^{*\text{T}} \Psi_{X_{n-1}}(X_{n-1}) + \varepsilon_{n-1}(X_{n-1}), |\varepsilon_{n-1}(X_{n-1})| < \bar{\varepsilon}_{n-1}$, where $\bar{\varepsilon}_i > 0$, and one can obtain

$$\begin{aligned} D^\alpha \chi_{n-1} &= W_{X_{n-1}}^{*\text{T}} \Psi_{X_{n-1}}(X_{n-1}) + \varepsilon_{n-1}(X_{n-1}) \\ &+ g_{n-1}(\bar{x}_{n-1}, \eta_{n-1} x_n)(\zeta_n + a_{n-1} - u_s(t)) + d_{n-1}(t) \end{aligned} \tag{28}$$

Select the Lyapunov function candidate $V_i = V_{i-1} + \frac{1}{2} \ln \frac{k_{b_i}^2}{k_{b_i}^2 - \chi_i^2} + \frac{g_{i \min}}{2\gamma_i} \tilde{\theta}_i^2 + \frac{g_{i \min}}{2\zeta_i} \tilde{\omega}_i^2 + \frac{1}{2} \zeta_i^2$, where $k_{b_{n-1}} > 0$ and its definition will be obtained later. $\gamma_{n-1} > 0$ and $\zeta_{n-1} > 0$ are the design parameters. $\tilde{\theta}_{n-1} = \theta_{n-1}^* - \theta_{n-1}$ is the parameter estimation error with the estimate θ_{n-1} of the parameter $\theta_{n-1}^* = \left\| W_{X_{n-1}}^* \right\|^2 / g_{n-1 \min}$. $\tilde{\omega}_{n-1} = \omega_{n-1}^* - \omega_{n-1}$ is the parameter estimation error with the upper bound $\omega_{n-1}^* = \tilde{\varepsilon}_{n-1}^2 + d_{n-1}^2$, and ω_{n-1} is the parameter estimation of ω_{n-1}^* .

Similar to the analysis in Step 1 using Young’s inequality yields:

$$\begin{aligned} & \frac{\chi_{n-1}}{k_{b_{n-1}}^2 - \chi_{n-1}^2} W_{X_{n-1}}^{*T} \Psi_{X_{n-1}}(X_{n-1}) \\ & \leq \frac{g_{n-1 \min} \chi_{n-1}^2}{2c_{n-1}^2 (k_{b_{n-1}}^2 - \chi_{n-1}^2)^2} \theta_{n-1}^* \left\| \Psi_{X_{n-1}}(X_{n-1}) \right\|^2 + \frac{c_{n-1}^2}{2} \end{aligned} \tag{29}$$

$$\frac{\chi_{n-1}}{k_{b_{n-1}}^2 - \chi_{n-1}^2} \varepsilon_{n-1}(X_{n-1}) \leq \frac{g_{n-1 \min} \tilde{\varepsilon}_{n-1}^2 \chi_{n-1}^2}{2\zeta_{n-1}^2 (k_{b_{n-1}}^2 - \chi_{n-1}^2)^2} + \frac{\zeta_{n-1}^2}{2g_{n-1 \min}} \tag{30}$$

$$\begin{aligned} & \frac{\chi_{n-1}}{k_{b_{n-1}}^2 - \chi_{n-1}^2} g_{n-1}(\bar{x}_{n-1}, \eta_{n-1} x_n) \zeta_n \\ & \leq \frac{g_{n-1 \min} \chi_{n-1}^2}{2\delta_{n-1}^2 (k_{b_{n-1}}^2 - \chi_{n-1}^2)^2} + \frac{\delta_{n-1}^2 g_{n-1 \max}^2}{2g_{n-1 \min}} \zeta_n^2 \end{aligned} \tag{31}$$

$$\frac{\chi_{n-1}}{k_{b_{n-1}}^2 - \chi_{n-1}^2} d_{n-1}(t) \leq \frac{g_{n-1 \min} d_{n-1}^2 \chi_{n-1}^2}{2\tilde{\zeta}_{n-1}^2 (k_{b_{n-1}}^2 - \chi_{n-1}^2)^2} + \frac{\tilde{\zeta}_{n-1}^2}{2g_{n-1 \min}} \tag{32}$$

where $c_{n-1}, \zeta_{n-1}, \delta_{n-1} > 0$.

Note that the term $u_s(t)$ can be viewed as a bounded signal according to (5). Therefore, the following inequality can be obtained

$$\begin{aligned} & -\frac{\chi_{n-1}}{k_{b_{n-1}}^2 - \chi_{n-1}^2} g_{n-1}(\bar{x}_{n-1}, \eta_{n-1} x_n) u_s(t) \\ & \leq \frac{g_{n-1 \min} \chi_{n-1}^2}{2\delta_{n-1}^2 (k_{b_{n-1}}^2 - \chi_{n-1}^2)^2} + \frac{\delta_{n-1}^2 g_{n-1 \max}^2}{2g_{n-1 \min}} \bar{u}_s^2 \end{aligned} \tag{33}$$

From (29) to (33) with Assumption 1, one can obtain

$$\begin{aligned} D^\alpha V_{n-1} & \leq D^\alpha V_{n-2} + \frac{\chi_{n-1}}{k_{b_{n-1}}^2 - \chi_{n-1}^2} g_{n-1}(\bar{x}_{n-1}, \eta_{n-1} x_n) a_{n-1} \\ & + \frac{g_{n-1 \min} \chi_{n-1}^2}{2c_{n-1}^2 (k_{b_{n-1}}^2 - \chi_{n-1}^2)^2} \theta_{n-1}^* \left\| \Psi_{X_{n-1}}(X_{n-1}) \right\|^2 \\ & + \frac{g_{n-1 \min} \omega_{n-1}^* \chi_{n-1}^2}{2\zeta_{n-1}^2 (k_{b_{n-1}}^2 - \chi_{n-1}^2)^2} + \frac{g_{n-1 \min} \chi_{n-1}^2}{\delta_{n-1}^2 (k_{b_{n-1}}^2 - \chi_{n-1}^2)^2} \\ & + \frac{c_{n-1}^2}{2} + \frac{\zeta_{n-1}^2}{2g_{n-1 \min}} + \frac{\delta_{n-1}^2 g_{n-1 \max}^2}{2g_{n-1 \min}} \zeta_n^2 + \frac{\delta_{n-1}^2 g_{n-1 \max}^2}{2g_{n-1 \min}} \bar{u}_s^2 \\ & - \frac{g_{n-1 \min}}{\gamma_{n-1}} \tilde{\theta}_{n-1} D^\alpha \theta_{n-1} - \frac{g_{n-1 \min}}{\zeta_{n-1}} \tilde{\omega}_{n-1} D^\alpha \omega_{n-1} + \zeta_{n-1} D^\alpha \zeta_{n-1} \end{aligned} \tag{34}$$

Design virtual controller a_{n-1} and adaptive laws as

$$a_{n-1} = -b_{n-1}\chi_{n-1} - \frac{\chi_{n-1}}{2c_{n-1}^2(k_{b_{n-1}}^2 - \chi_{n-1}^2)} \|\Psi_{X_{n-1}}(X_{n-1})\|^2 \theta_{n-1} - \frac{\chi_{n-1}}{2\zeta_{n-1}^2(k_{b_{n-1}}^2 - \chi_{n-1}^2)} \omega_{n-1} - \frac{\chi_{n-1}}{\delta_{n-1}^2(k_{b_{n-1}}^2 - \chi_{n-1}^2)} \tag{35}$$

$$D^\alpha \theta_{n-1} = \frac{\gamma_{n-1}\chi_{n-1}^2}{2c_{n-1}^2(k_{b_{n-1}}^2 - \chi_{n-1}^2)^2} \|\Psi_{X_{n-1}}(X_{n-1})\|^2 - \phi_{n-1}\theta_{n-1} \tag{36}$$

$$D^\alpha \omega_{n-1} = \frac{\zeta_{n-1}\chi_{n-1}^2}{2\zeta_{n-1}^2(k_{b_{n-1}}^2 - \chi_{n-1}^2)^2} - \varphi_{n-1}\omega_{n-1} \tag{37}$$

where $b_{n-1} > 0, \gamma_{n-1} > 0, \zeta_{n-1} > 0, \phi_{n-1} > 0$ and $\varphi_{n-1} > 0$ are the tunable parameters. Based on (35)–(37), (34) can be described as

$$\begin{aligned} D^\alpha V_{n-1} &\leq D^\alpha V_{n-2} - \frac{g_{n-1} \min b_{n-1} \chi_{n-1}^2}{k_{b_{n-1}}^2 - \chi_{n-1}^2} + \frac{c_{n-1}^2}{2} \\ &+ \frac{\delta_{n-1}^2 g_{n-1} \max}{2g_{n-1} \min} \zeta_n^2 + \frac{g_{n-1} \min}{\gamma_{n-1}} \phi_{n-1} \tilde{\theta}_{n-1} \theta_{n-1} + \zeta_{n-1} D^\alpha \zeta_{n-1} \\ &- \frac{g_{n-1} \min}{\zeta_{n-1}} \varphi_{n-1} \tilde{\omega}_{n-1} \omega_{n-1} + \frac{\zeta_{n-1}^2}{g_{n-1} \min} + \frac{\delta_{n-1}^2 g_{n-1} \max}{2g_{n-1} \min} \bar{u}_s^2 \\ &\leq - \sum_{i=1}^{n-1} \frac{b_i g_i \min \chi_i^2}{k_{b_i}^2 - \chi_i^2} + \sum_{i=1}^{n-1} \frac{\zeta_i^2}{g_i \min} + \sum_{i=1}^{n-1} \frac{\delta_i^2 g_i \max}{2g_i \min} \zeta_{i+1}^2 \\ &+ \sum_{i=1}^{n-1} \frac{g_i \min}{\gamma_i} \phi_i \tilde{\theta}_i \theta_i + \sum_{i=1}^{n-1} \frac{g_i \min}{\zeta_i} \varphi_i \tilde{\omega}_i \omega_i \\ &+ \sum_{i=2}^{n-1} \zeta_i D^\alpha \zeta_i + \sum_{i=1}^{n-1} \frac{c_i^2}{2} + \frac{\delta_{n-1}^2 g_{n-1} \max}{2g_{n-1} \min} \bar{u}_s^2 \end{aligned} \tag{38}$$

Step n : T derivative of χ_n is derived as

$$\begin{aligned} D^\alpha \chi_n &= D^\alpha x_n - D^\alpha a_{n,l} + u(v(t)) - u(v(t - \tau)) \\ &= f_n(\bar{x}_n) - D^\alpha a_{n,l} + h_{v_\mu} v + \Delta(v) + d_n(t) \end{aligned} \tag{39}$$

where $F_n(X_n) = f_n(\bar{x}_n) - D^\alpha a_{n,l}$ is approximated via the RBFNN $W_{X_n}^{*T} \Psi_{X_n}(X_n)$, and $W_{X_n}^*$ is the optimal parameter vector satisfying $F_n(X_n) = W_{X_n}^{*T} \Psi_{X_n}(X_n) + \varepsilon_n(X_n)$. Assume that $\exists \bar{\varepsilon}_n > 0$ such that $|\varepsilon_n(X_n)| < \bar{\varepsilon}_n$. Then, (39) can be described as $D^\alpha \chi_n = W_{X_n}^{*T} \Psi_{X_n}(X_n) + \varepsilon_n(X_n) + h_{v_\mu} v + \Delta(v) + d_n(t)$.

Select the Lyapunov candidate function $V_n = V_{n-1} + \frac{1}{2} \ln \frac{k_{b_n}^2}{k_{b_n}^2 - \chi_n^2} + \frac{h_{\min}}{2\gamma_n} \tilde{\theta}_n^2 + \frac{h_{\min}}{2\zeta_n} \tilde{\omega}_n^2 + \frac{1}{2} \zeta_n^2$, where $k_{b_n} > 0$ and its definition will be obtained later. $\gamma_n > 0$ and $\zeta_n > 0$ are the design parameters. $\tilde{\theta}_n = \theta_n^* - \theta_n$ is the parameter estimation error with the estimate θ_n of the parameter $\theta_n^* = \|W_{X_n}^*\|^2 / h_{\min}$. $\tilde{\omega}_n = \omega_n^* - \omega_n$ is the parameter estimation error with the upper bound $\omega_n^* = \bar{\varepsilon}_n^2 + \bar{d}_n^2 + \bar{D}^2$, and ω_n is the parameter estimation of ω_n^* . Compute the fractional-order derivative of V_n

$$\begin{aligned} D^\alpha V_n &= D^\alpha V_{n-1} + \frac{\chi_n}{k_{b_n}^2 - \chi_n^2} \left(W_{X_n}^{*T} \Psi_{X_n}(X_n) + \varepsilon_n(X_n) \right) \\ &+ \frac{\chi_n}{k_{b_n}^2 - \chi_n^2} \left(h_{v_\mu} v + \Delta(v) + d_n(t) \right) \\ &- \frac{h_{\min}}{\gamma_n} \tilde{\theta}_n D^\alpha \theta_n - \frac{h_{\min}}{\zeta_n} \tilde{\omega}_n D^\alpha \omega_n + \zeta_n D^\alpha \zeta_n \end{aligned} \tag{40}$$

By employing Young’s inequality with Assumption 1, one has

$$\frac{\chi_n}{k_{b_n}^2 - \chi_n^2} W_{X_n}^{*\Gamma} \Psi_{X_n}(X_n) \leq \frac{h_{\min} \chi_n^2}{2c_n^2 (k_{b_n}^2 - \chi_n^2)} \theta_n^* \|\Psi_{X_n}(X_n)\|^2 + \frac{c_n^2}{2} \tag{41}$$

$$\frac{\chi_n}{k_{b_n}^2 - \chi_n^2} \varepsilon_n(X_n) \leq \frac{h_{\min} \bar{\varepsilon}_n^2 \chi_n^2}{2\bar{\xi}_n^2 (k_{b_n}^2 - \chi_n^2)} + \frac{\bar{\xi}_n^2}{2h_{\min}} \tag{42}$$

$$\frac{\chi_n}{k_{b_n}^2 - \chi_n^2} \Delta(v) \leq \frac{h_{\min} \bar{D}_n^2 \chi_n^2}{2\bar{\xi}_n^2 (k_{b_n}^2 - \chi_n^2)} + \frac{\bar{\xi}_n^2}{2h_{\min}} \tag{43}$$

$$\frac{\chi_n}{k_{b_n}^2 - \chi_n^2} d_n(t) \leq \frac{h_{\min} \bar{d}_n^2 \chi_n^2}{2\bar{\xi}_n^2 (k_{b_n}^2 - \chi_n^2)} + \frac{\bar{\xi}_n^2}{2h_{\min}} \tag{44}$$

where $c_n, \bar{\xi}_n, \delta_n > 0$.

Substituting (41)–(44) into (40) yields

$$\begin{aligned} D^\alpha V_n &\leq D^\alpha V_{n-1} + \frac{\chi_n}{k_{b_n}^2 - \chi_n^2} h_{v_\mu} v \\ &+ \frac{h_{\min} \chi_n^2}{2c_n^2 (k_{b_n}^2 - \chi_n^2)} \theta_n^* \|\Psi_{X_n}(X_n)\|^2 + \frac{h_{\min} \omega_n^* \chi_n^2}{2\bar{\xi}_n^2 (k_{b_n}^2 - \chi_n^2)} \\ &- \frac{h_{\min} \bar{\theta}_n D^\alpha \theta_n}{\gamma_n} - \frac{h_{\min} \bar{\omega}_n D^\alpha \omega_n}{\zeta_n} + \zeta_n D^\alpha \zeta_n + \frac{c_n^2}{2} + \frac{3\bar{\xi}_n^2}{h_{\min}} \\ &\leq D^\alpha V_{n-1} - \frac{h_{\min}}{\zeta_n} \bar{\omega}_n \left(D^\alpha \omega_n - \frac{\zeta_n \chi_n^2}{\bar{\xi}_n^2 (k_{b_n}^2 - \chi_n^2)} \right) \\ &+ \frac{\chi_n}{k_{b_n}^2 - \chi_n^2} \left(h_{v_\mu} v + \frac{h_{\min} \chi_n \theta_n \|\Psi_{X_n}(X_n)\|^2}{2c_n^2 (k_{b_n}^2 - \chi_n^2)} + \frac{h_{\min} \chi_n \omega_n}{\bar{\xi}_n^2 (k_{b_n}^2 - \chi_n^2)} \right) \\ &- \frac{h_{\min} \bar{\theta}_n}{\gamma_n} \left(D^\alpha \theta_n - \frac{\gamma_n \chi_n^2}{2c_n^2 (k_{b_n}^2 - \chi_n^2)} \|\Psi_{X_n}(X_n)\|^2 \right) \\ &+ \zeta_n D^\alpha \zeta_n + 2c_n^2 + \frac{3\bar{\xi}_n^2}{h_{\min}} \end{aligned} \tag{45}$$

Design the fractional-order adaptive laws as

$$D^\alpha \theta_n = \frac{\gamma_n \chi_n^2}{2c_n^2 (k_{b_n}^2 - \chi_n^2)} \|\Psi_{X_n}(X_n)\|^2 - \phi_n \theta_n \tag{46}$$

$$D^\alpha \omega_n = \frac{\zeta_n \chi_n^2}{2\bar{\xi}_n^2 (k_{b_n}^2 - \chi_n^2)} - \varphi_n \omega_n \tag{47}$$

where $\gamma_n > 0, \zeta_n > 0, \phi_n > 0$ and $\varphi_n > 0$ are the tunable parameters.

Design event-triggered controller as

$$v(t) = \Theta(t_k), \forall t \in [t_k, t_{k+1}) \tag{48}$$

$$\Theta(t) = -(1 + \lambda_1^*) \left(a_n \tanh \left(\frac{a_n \chi_n}{\kappa^* (k_{b_n}^2 - \chi_n^2)} \right) + \bar{\lambda}_2^* \tanh \left(\frac{\bar{\lambda}_2^* \chi_n}{\kappa^* (k_{b_n}^2 - \chi_n^2)} \right) \right) \tag{49}$$

$$a_n = b_n \chi_n + \frac{\chi_n}{2\zeta_n^2 (k_{b_n}^2 - \chi_n^2)} \omega_n + \frac{\chi_n}{2c_n^2 (k_{b_n}^2 - \chi_n^2)} \theta_n \|\Psi_{X_n}(X_n)\|^2 \tag{50}$$

where $b_n > 0$ and $\kappa^* > 0$ are the tunable parameters. The sampling instants are determined by the following triggering condition

$$t_{k+1} = \inf\{t \in \mathbb{R} \mid |Y(t)| \geq \lambda_1^* |v(t)| + \lambda_2^*\} \tag{51}$$

where $t_k (k \in \mathbb{Z}^+)$ is the controller update time. $\lambda_1^* \in (0, 1)$, $\bar{\lambda}_2^* > \frac{\lambda_2^*}{1-\lambda_1^*}$ and $\lambda_2^* > 0$ are known parameters.

Define event sampling error $Y(t) = \Theta(t) - v(t)$, together with (51), we have

$$\Theta(t) = (1 + \lambda_1^* \lambda_1(t))v(t) + \lambda_2^* \lambda_2(t) \tag{52}$$

where $|\lambda_1(t)| \leq 1$ and $|\lambda_2(t)| \leq 1$. In view of $|\lambda_1(t)| \leq 1$ and $|\lambda_2(t)| \leq 1$, we obtain

$$\frac{\Theta(t)\chi_n}{1 + \lambda_1^* \lambda_1(t)} \leq \frac{\Theta(t)\chi_n}{1 + \lambda_1^*} \tag{53}$$

$$\frac{\lambda_2^* \lambda_2(t)}{1 + \lambda_1^* \lambda_1(t)} \leq \left| \frac{\lambda_2^*}{1 - \lambda_1^*} \right|$$

Substituting (46)–(53) into (45), we obtain

$$\begin{aligned} D^\alpha V_n &\leq D^\alpha V_{n-1} + \frac{h_{v_n} \chi_n}{k_{b_n}^2 - \chi_n^2} \frac{\Theta(t)}{1 + \lambda_1^* \lambda_1(t)} - \frac{h_{v_n} \chi_n}{k_{b_n}^2 - \chi_n^2} \frac{\lambda_2^* \lambda_2(t)}{1 + \lambda_1^* \lambda_1(t)} \\ &+ \frac{\chi_n}{k_{b_n}^2 - \chi_n^2} \left(\frac{h_{\min} \chi_n}{2c_n^2 (k_{b_n}^2 - \chi_n^2)} \theta_n \|\Psi_{X_n}(X_n)\|^2 + \frac{h_{\min} \chi_n}{\zeta_n^2 (k_{b_n}^2 - \chi_n^2)} \omega_n \right) \\ &+ \frac{h_{\min} \phi_n}{\gamma_n} \bar{\theta}_n \theta_n + \frac{h_{\min} \varphi_n}{\zeta_n} \bar{\omega}_n \omega_n + \zeta_n D^\alpha \zeta_n + 2c_n^2 + \frac{3\zeta_n^2}{h_{\min}} \\ &\leq D^\alpha V_{n-1} - \frac{h_{v_n} \chi_n}{k_{b_n}^2 - \chi_n^2} \frac{\lambda_2^* \lambda_2(t)}{1 + \lambda_1^* \lambda_1(t)} \\ &- \frac{(1 + \lambda_1^*)}{1 + \lambda_1^* \lambda_1(t)} \frac{h_{v_n} a_n \chi_n}{k_{b_n}^2 - \chi_n^2} \tanh\left(\frac{a_n \chi_n}{\kappa^* (k_{b_n}^2 - \chi_n^2)}\right) \\ &- \frac{(1 + \lambda_1^*)}{1 + \lambda_1^* \lambda_1(t)} \frac{h_{v_n} \bar{\lambda}_2^* \chi_n}{k_{b_n}^2 - \chi_n^2} \tanh\left(\frac{\bar{\lambda}_2^* \chi_n}{\kappa^* (k_{b_n}^2 - \chi_n^2)}\right) \\ &+ \frac{\chi_n}{k_{b_n}^2 - \chi_n^2} \left(\frac{h_{\min} \chi_n}{2c_n^2 (k_{b_n}^2 - \chi_n^2)} \theta_n \|\Psi_{X_n}(X_n)\|^2 + \frac{h_{\min} \chi_n}{\zeta_n^2 (k_{b_n}^2 - \chi_n^2)} \omega_n \right) \\ &+ \frac{h_{\min} \phi_n}{\gamma_n} \bar{\theta}_n \theta_n + \frac{h_{\min} \varphi_n}{\zeta_n} \bar{\omega}_n \omega_n + \zeta_n D^\alpha \zeta_n + 2c_n^2 + \frac{3\zeta_n^2}{h_{\min}} \tag{54} \\ &\leq D^\alpha V_{n-1} + \frac{h_{\min} \phi_n}{\gamma_n} \bar{\theta}_n \theta_n + \frac{h_{\min} \varphi_n}{\zeta_n} \bar{\omega}_n \omega_n + \zeta_n D^\alpha \zeta_n + 2c_n^2 + \frac{3\zeta_n^2}{h_{\min}} \\ &+ \frac{\chi_n}{k_{b_n}^2 - \chi_n^2} \left(-h_{v_n} a_n + \frac{h_{\min} \chi_n}{2c_n^2 (k_{b_n}^2 - \chi_n^2)} \theta_n \|\Psi_{X_n}(X_n)\|^2 + \frac{h_{\min} \chi_n}{\zeta_n^2 (k_{b_n}^2 - \chi_n^2)} \omega_n \right) \\ &+ \sum_{i=1}^{n-1} \frac{g_i \min}{\gamma_i} \phi_i \bar{\theta}_i \theta_i + \frac{h_{\min}}{\gamma_n} \phi_n \bar{\theta}_n \theta_n + \sum_{i=1}^{n-1} \frac{g_i \min}{\zeta_i} \varphi_i \bar{\omega}_i \omega_i \\ &+ \frac{h_{\min}}{\zeta_n} \varphi_n \bar{\omega}_n \omega_n + \sum_{i=2}^n \zeta_i D^\alpha \zeta_i + 0.557 \kappa^* \\ &\leq - \sum_{i=1}^{n-1} \frac{b_i g_i \min \chi_i^2}{k_{b_i}^2 - \chi_i^2} - \frac{h_{\min} b_n \chi_n^2}{k_{b_n}^2 - \chi_n^2} + \sum_{i=1}^{n-1} \frac{2\zeta_i^2}{g_i \min} \\ &+ \frac{3\zeta_n^2}{h_{\min}} + \sum_{i=1}^n 2c_i^2 + \sum_{i=1}^{n-1} \frac{\delta_i^2 g_i \max}{2g_i \min} \zeta_{i+1}^2 + \frac{\delta_{n-1}^2 g_{n-1} \max}{2g_{n-1} \min} \zeta_n^2 \\ &+ \sum_{i=1}^{n-1} \frac{g_i \min}{\gamma_i} \phi_i \bar{\theta}_i \theta_i + \frac{h_{\min}}{\gamma_n} \phi_n \bar{\theta}_n \theta_n + \sum_{i=1}^{n-1} \frac{g_i \min}{\zeta_i} \varphi_i \bar{\omega}_i \omega_i \\ &+ \frac{h_{\min}}{\zeta_n} \varphi_n \bar{\omega}_n \omega_n + \sum_{i=2}^n \zeta_i D^\alpha \zeta_i + 0.557 \kappa^* \end{aligned}$$

4.2. Stability Analysis

Theorem 1. Considering the pure-feedback FONSS (2) under Assumptions 1–3, virtual control functions (14), (24) and (35), fractional-order adaptive laws (15), (16), (25), (26), (36), (37), (46) and (47), and the event-triggered adaptive controller presented in (48)–(51), the following holds (The proof of Theorem 1 see Appendix A):

(i) All system signals are bounded, and error signal χ_i will stay around the compact set

$$\Omega_\chi = \left\{ \chi_i \mid |\chi_i| \leq k_{b_k} \sqrt{1 - e^{-2V_n(0)E_{(\alpha,1)}(-\rho t^\alpha) - 2M\theta/\rho}}, i = 1, \dots, n \right\} \quad (55)$$

(ii) All system states can not transgress the sets.

(iii) The Zeno behavior can be avoided.

5. Simulation

5.1. Example 1

A two-order pure-feedback FONS with full state constraints is described as

$$\begin{cases} D^{0.6}x_1 = -0.5x_1^2 + x_2 + 0.01 \sin(t) \\ D^{0.6}x_2 = \frac{x_2 - 0.3x_1^2}{1 + 0.5x_1^4} - x_2 + u(v(t - \tau)) + 0.05 \cos(t) \end{cases}$$

where $f_1(x_1, x_2) = -0.5x_1^2 + x_2$, $f_2(x_1, x_2) = \frac{x_2 - 0.3x_1^2}{1 + 0.5x_1^4} - x_2$, $\tau = 0.01$, $d_1(t) = 0.01 \sin(t)$ and $d_2(t) = 0.05 \cos(t)$. x_1 and x_2 are the system states, which are confined as $|x_1| \leq k_{c_1} = 0.8$ and $|x_2| \leq k_{c_2} = 0.6$, respectively, and $y_r(t) = 0.5 \sin(t)$. v and $u(v)$ are the saturation input and output, and the saturation parameters are $u_{\max} = 0.8$ and $u_{\min} = -0.5$.

Using the adaptive controller (14) and (48)–(51) with parameter-updated laws (15), (16), (46) and (47), the design parameters are chosen as $b_1 = 25$, $b_2 = 8$, $c_1 = 11$, $c_2 = 113$, $\phi_1 = \phi_2 = 1.01$, $\gamma_1 = 1.001$, $\gamma_2 = 1.101$, $\xi_1 = 11$, $\xi_2 = 111.1$, $\delta_1 = 1.1$, $\varphi_1 = \varphi_2 = \zeta_1 = \zeta_2 = 1.1$, $\kappa_2 = 0.06$, $\kappa^* = 0.01$, $\lambda_1^* = 0.001$, $\lambda_2^* = 0.1$ and $\bar{\lambda}_2^* = 0.2001$. Meanwhile, the initial values are selected as $x_1(0) = x_2(0) = 0$, $\theta_1(0) = \theta_2(0) = 0$ and $\omega_1(0) = \omega_2(0) = 0$.

The simulation results are shown by Figures 2–8. Figure 2 displays output tracking trajectories between the system output y and the reference signal y_r . Figure 3 shows the system states x_2 . It is clear from these figures the full state constraints are not violated. The control input signals u shown in Figure 4, adaptive estimation for θ_1 and θ_2 shown in Figure 5, and ω_1 and ω_2 shown in Figure 6 are all bounded. Figure 7 lists the sequence of steps of event-triggered sampling to demonstrate the time interval results of the triggering events, and Figure 8 shows the number of accumulated events according to the event-triggered sampling in Figure 7, which can display that the proposed event-triggered controller can reduce the computational burden.

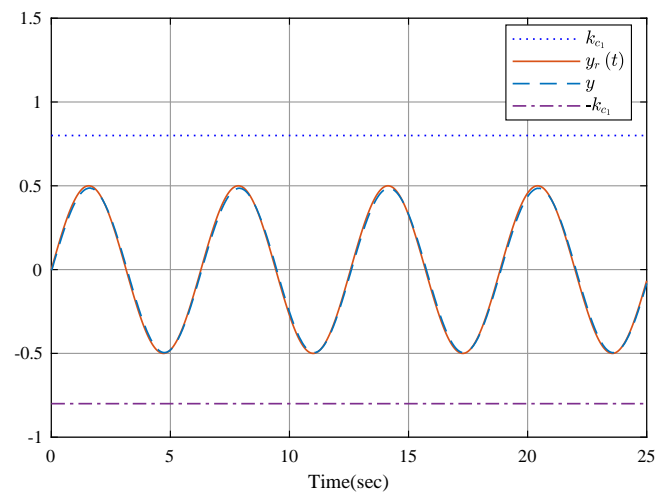


Figure 2. Output y and tracking signal $y_r(t)$.

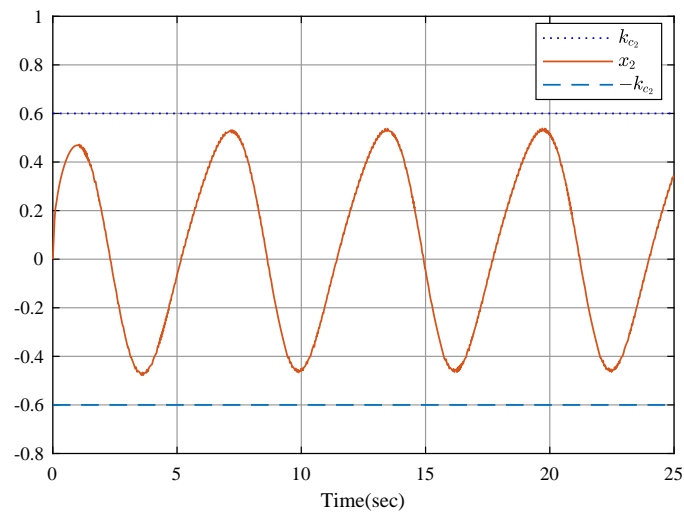


Figure 3. State x_2 .

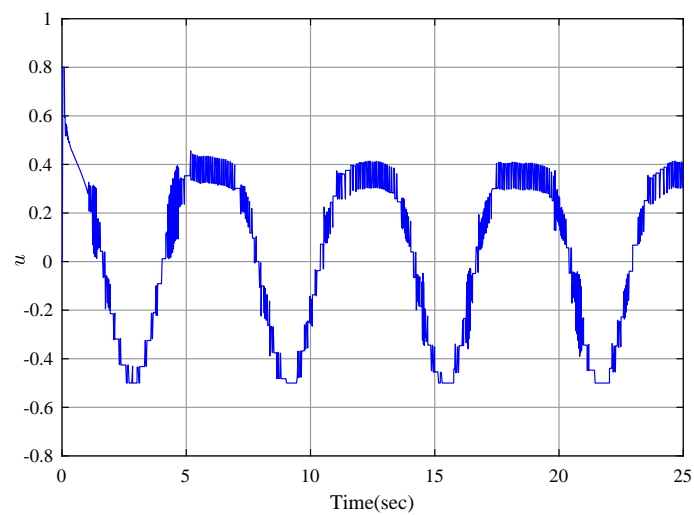


Figure 4. Control input u .

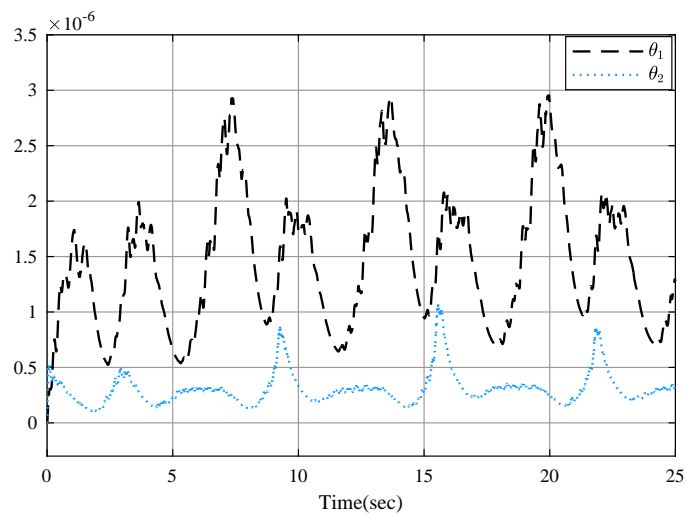


Figure 5. Parameter estimation θ_1 and θ_2 .

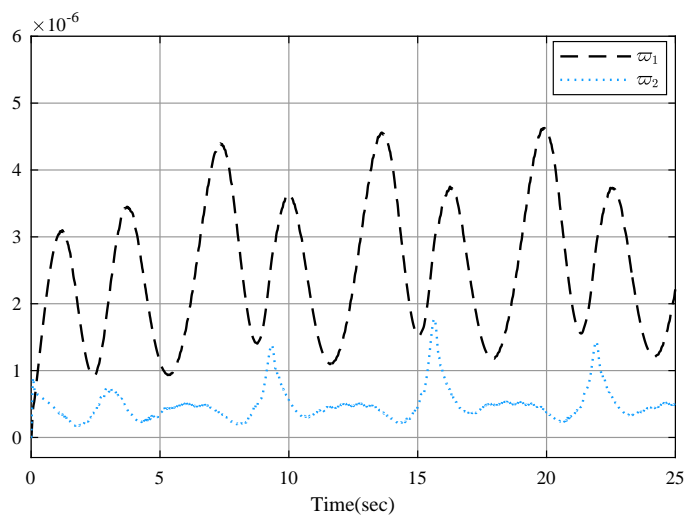


Figure 6. Parameter estimation ω_1 and ω_2 .

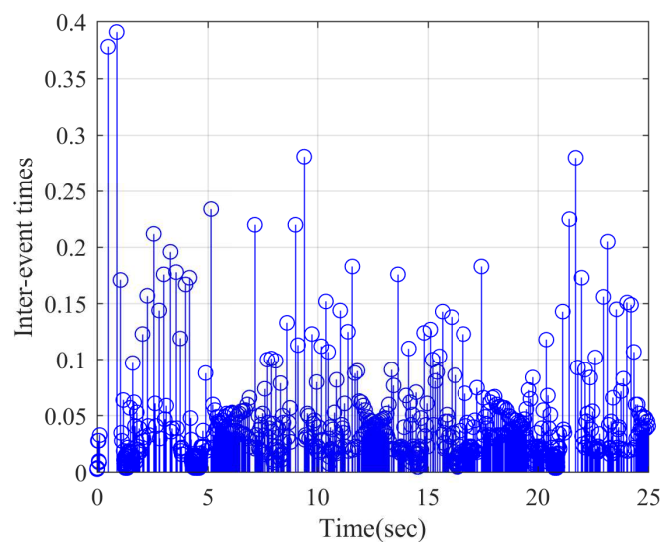


Figure 7. Time interval.

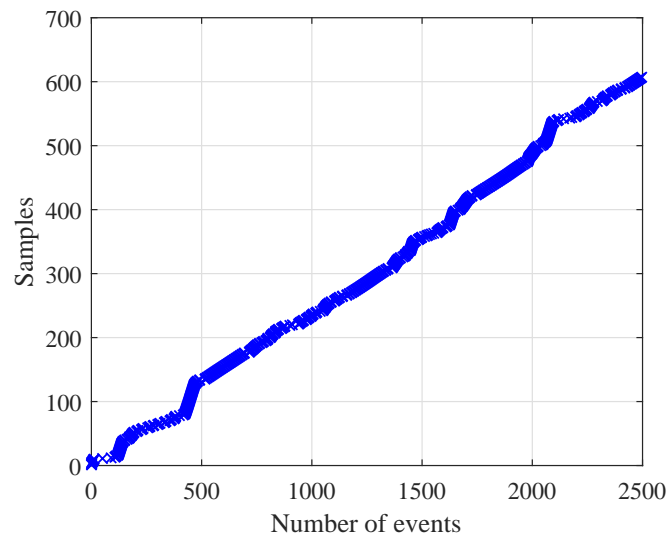


Figure 8. Cumulative number of events.

5.2. Example 2

In this example, the fractional-order Chua–Hartley system as a practical example is presented as follows [50]:

$$\begin{cases} D^\alpha x_1 = \frac{10}{7}(x_1 - x_1^3) + x_2 + d_1(t) \\ D^\alpha x_2 = 10x_1 - x_2 + x_3 + d_2(t) \\ D^\alpha x_3 = -\frac{100}{7}x_2 + u(v(t - \tau)) + d_3(t) \end{cases}$$

where $\alpha = 0.98$, $f_1(x_1, x_2) = x_2 + \frac{10}{7}(x_1 - x_1^3)$, $f_2(x_2, x_3) = 10x_1 - x_2 + x_3$, $f_3(x_3) = -\frac{100}{7}x_2$, and $\tau = 0.005$. $d_1(t) = 0.05 \cos(t)$, $d_2(t) = 0.1 \sin(t)$, and $d_3(t) = 0.01(\sin(t) + \cos(t))$ are the external disturbances. x_1, x_2 , and x_3 are the system states, which are confined as $|x_1| \leq k_{c1} = 0.9$, $|x_2| \leq k_{c2} = 1.6$, and $|x_3| \leq k_{c3} = 16$, respectively, and the desired signal is taken as $y_r(t) = 0.8 \sin(t)$. The saturation parameters are $u_{\max} = 200$ and $u_{\min} = -210$.

The design parameters are chosen as $b_1 = 16.1$, $b_2 = 31.1$, $b_3 = 71.1$, $c_1 = 1.1$, $c_2 = c_3 = 101.8$, $\phi_1 = \phi_2 = \phi_3 = 1.01$, $\gamma_1 = \gamma_2 = \gamma_3 = 0.001$, $\zeta_1 = 11.1$, $\zeta_2 = \zeta_3 = 101.1$, $\delta_1 = \delta_2 = 1$, $\varphi_1 = \varphi_2 = \varphi_3 = 1.1$, $\varsigma_1 = \varsigma_2 = \varsigma_3 = 0.01$, $\kappa_2 = \kappa_3 = 0.01$, $\kappa^* = 0.01$, $\lambda_1^* = 0.001$, $\lambda_2^* = 1.1$, and $\bar{\lambda}_2^* = 1.2011$. Meanwhile, the initial values are selected as $x_1(0) = x_2(0) = x_3(0) = 0$, $\theta_1(0) = \theta_2(0) = \theta_3(0) = 0$, and $\omega_1(0) = \omega_2(0) = \omega_3(0) = 0$.

To show the advantages of the proposed controller, a robust adaptive backstepping controller (RABC) in [52] is employed. Figure 9 shows the position relationship of y and y_r , in which the constraints are not violated. State x_2 is shown in Figures 10 and 11, and x_3 is displayed in Figures 12 and 13 by RABC and the proposed scheme, respectively. It is clear that the system states x_2 and x_3 by the proposed scheme satisfy the constraints $x_2 < 1.6$ and $x_3 < 16$. However, the system state x_2 and x_3 by the RABC violate the preset state constraints. The control input signals u shown in Figure 14, adaptive estimation for θ_1, θ_2 , and θ_3 shown in Figure 15, and ω_1, ω_2 , and ω_3 shown in Figure 16 are all bounded. Figures 17 and 18 show the sequence of steps of event-triggered sampling and the number of accumulated events to demonstrate the effectiveness of the computational burden reduction.

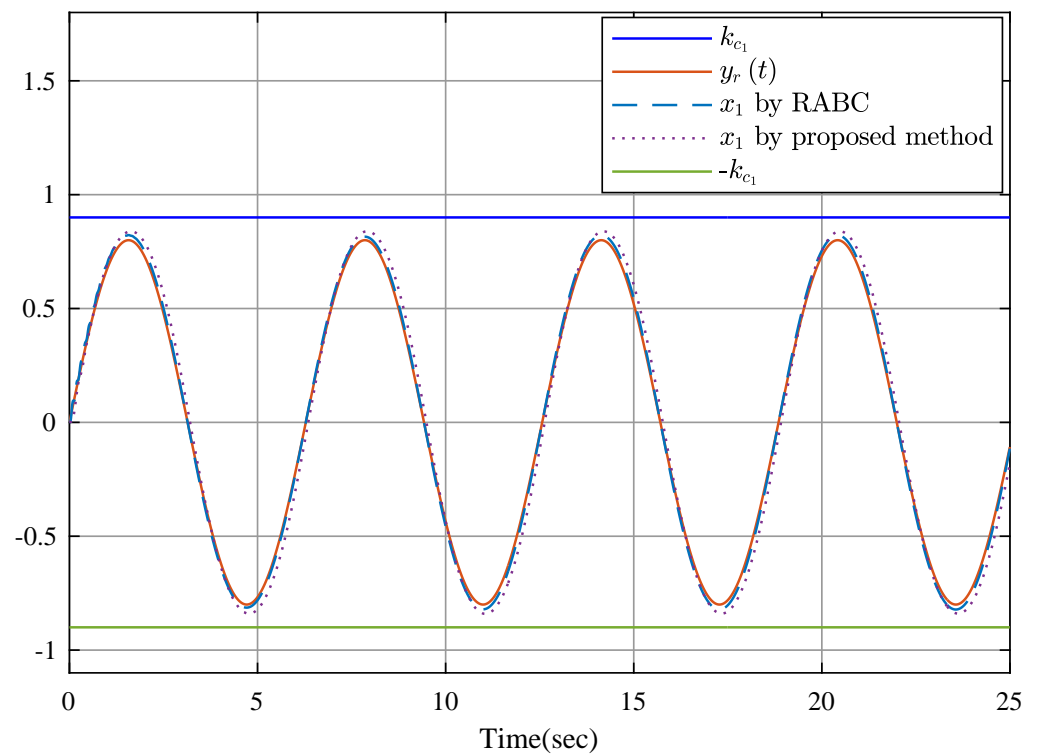


Figure 9. Output y and tracking signal $y_r(t)$.

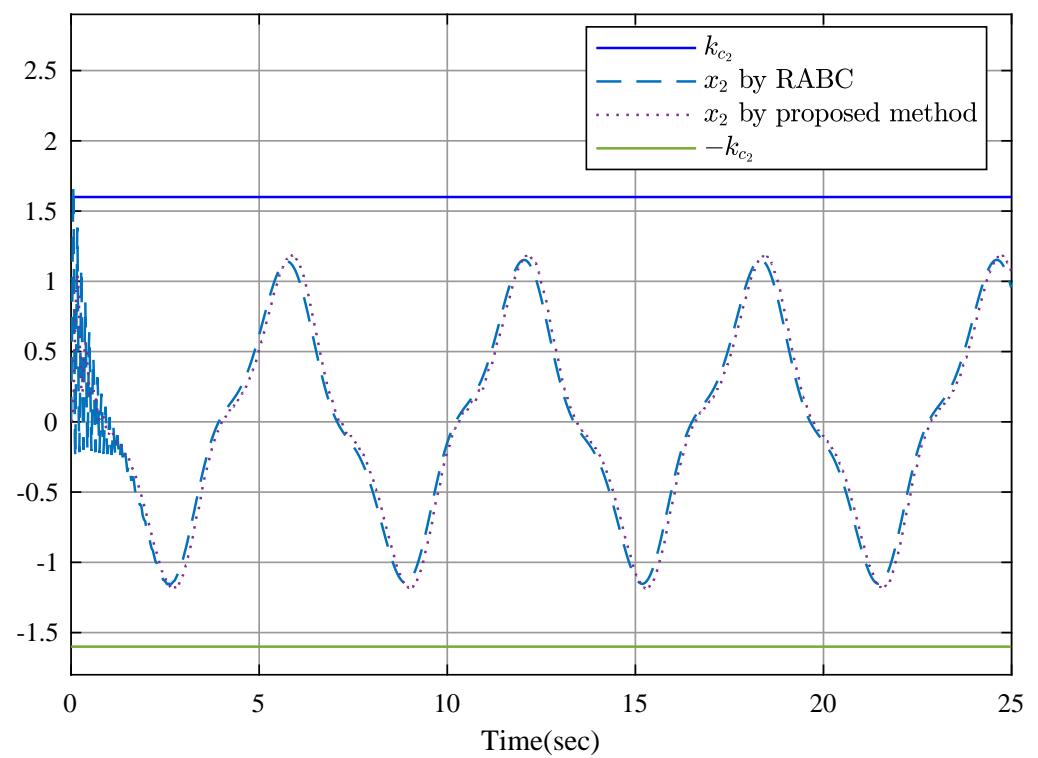
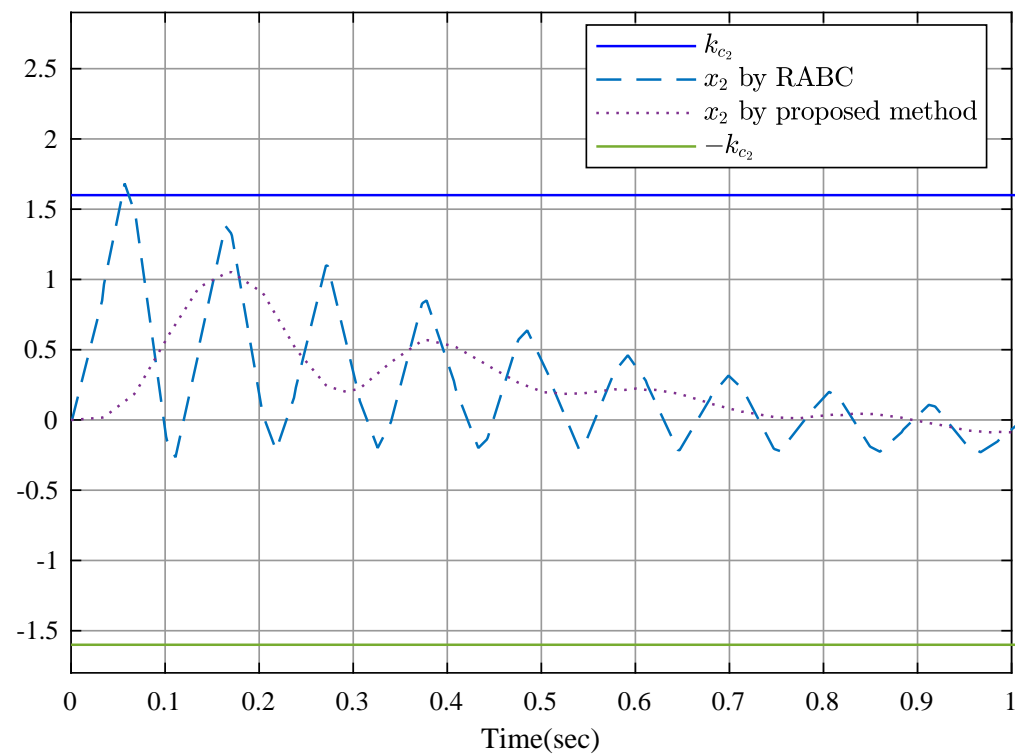
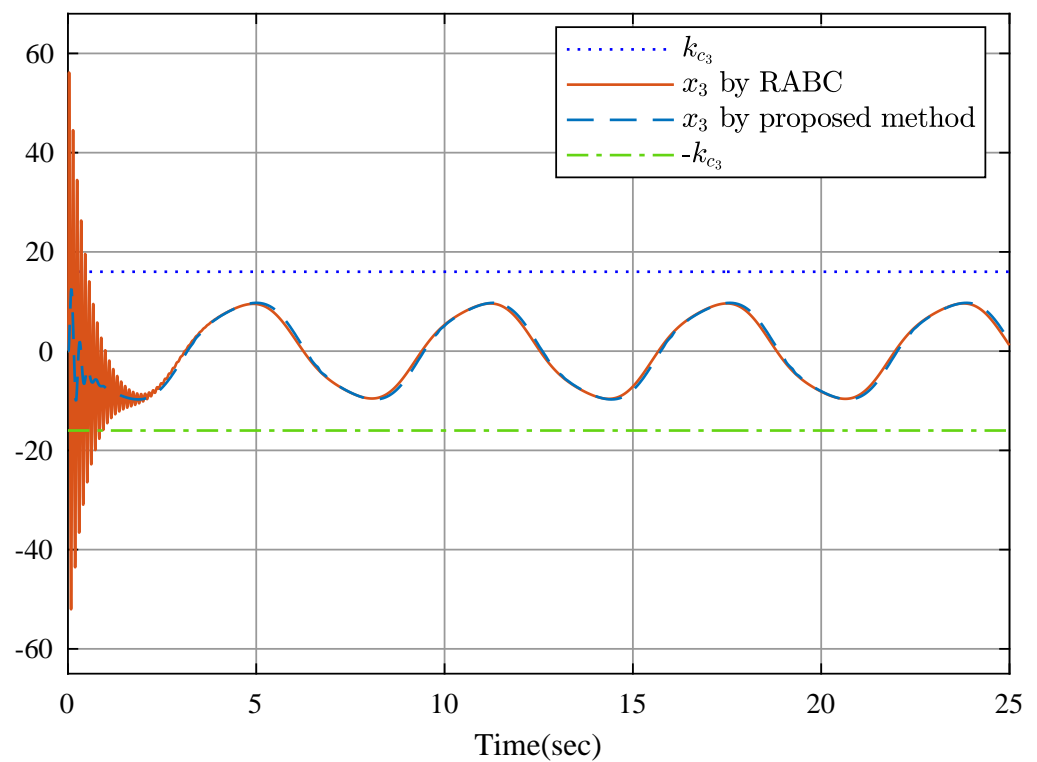


Figure 10. State x_2 .

Figure 11. State x_2 .Figure 12. State x_3 .

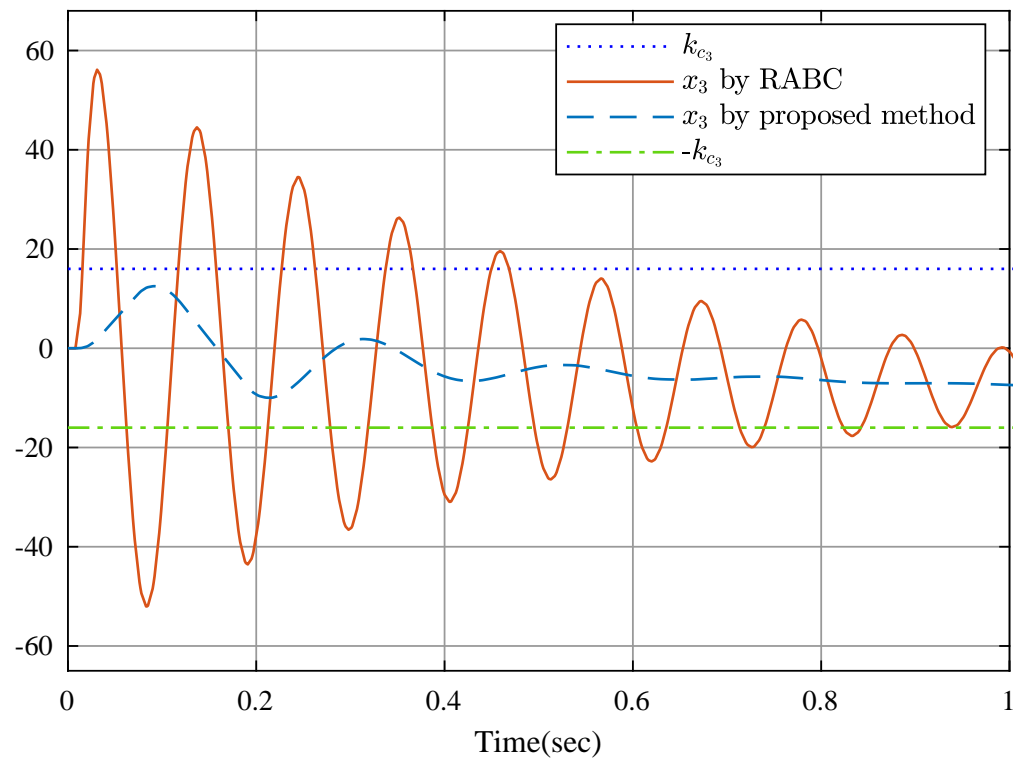


Figure 13. State x_3 .

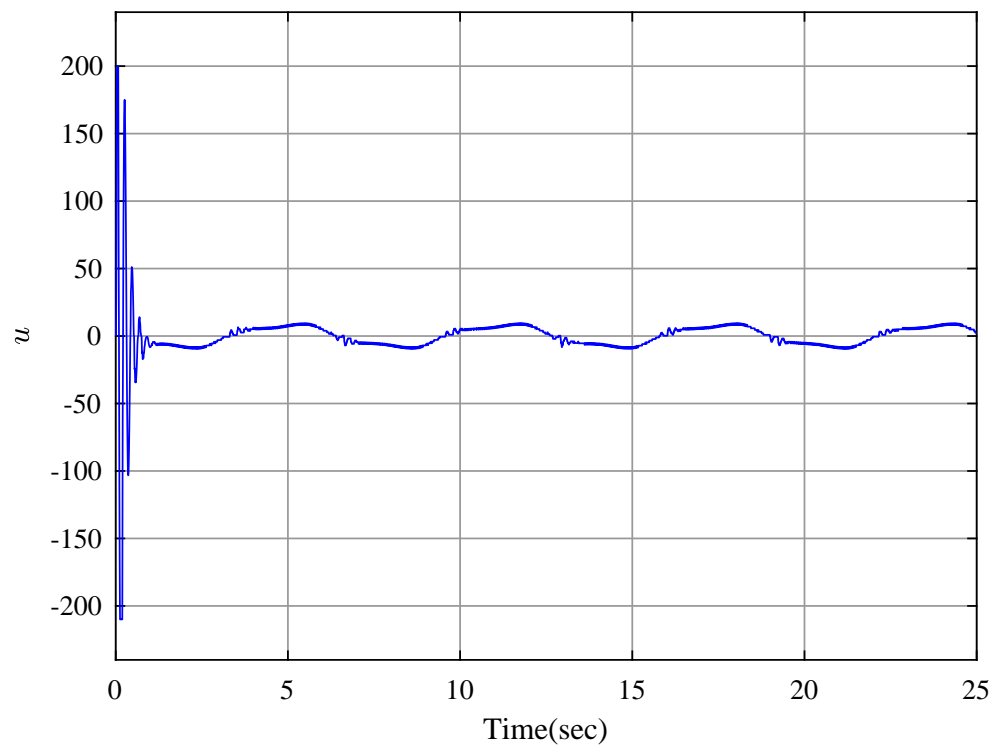


Figure 14. Control input u .

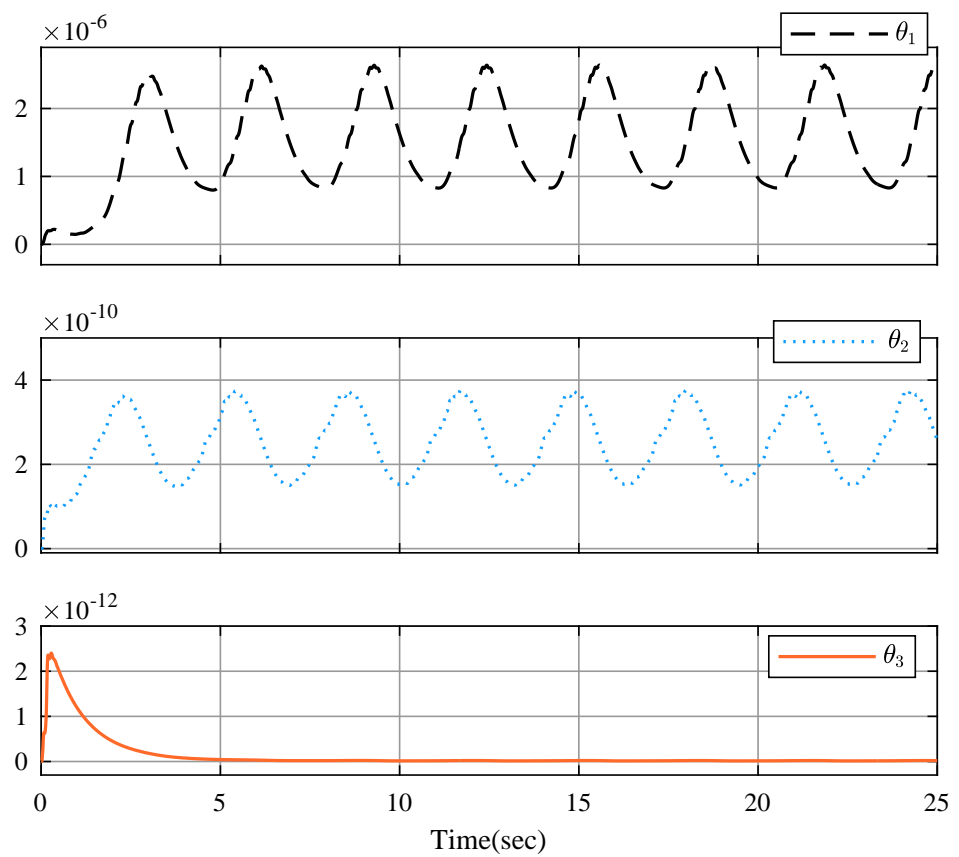


Figure 15. Parameter estimation θ_1, θ_2 , and θ_3 .

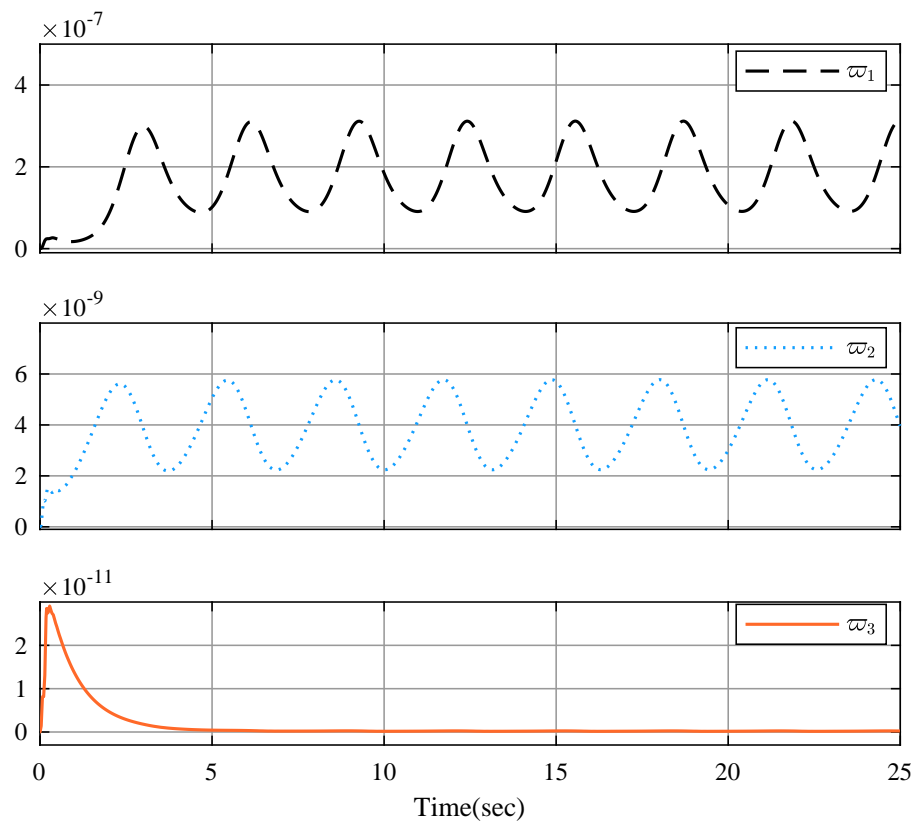


Figure 16. Parameter estimation ω_1, ω_2 , and ω_3 .

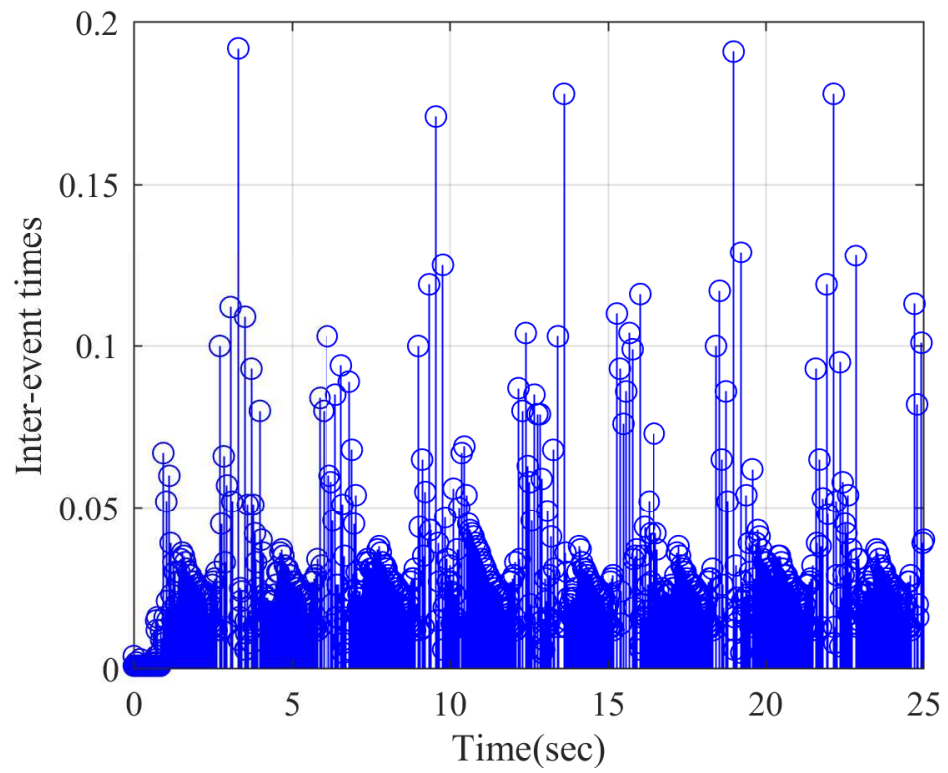


Figure 17. Time interval.

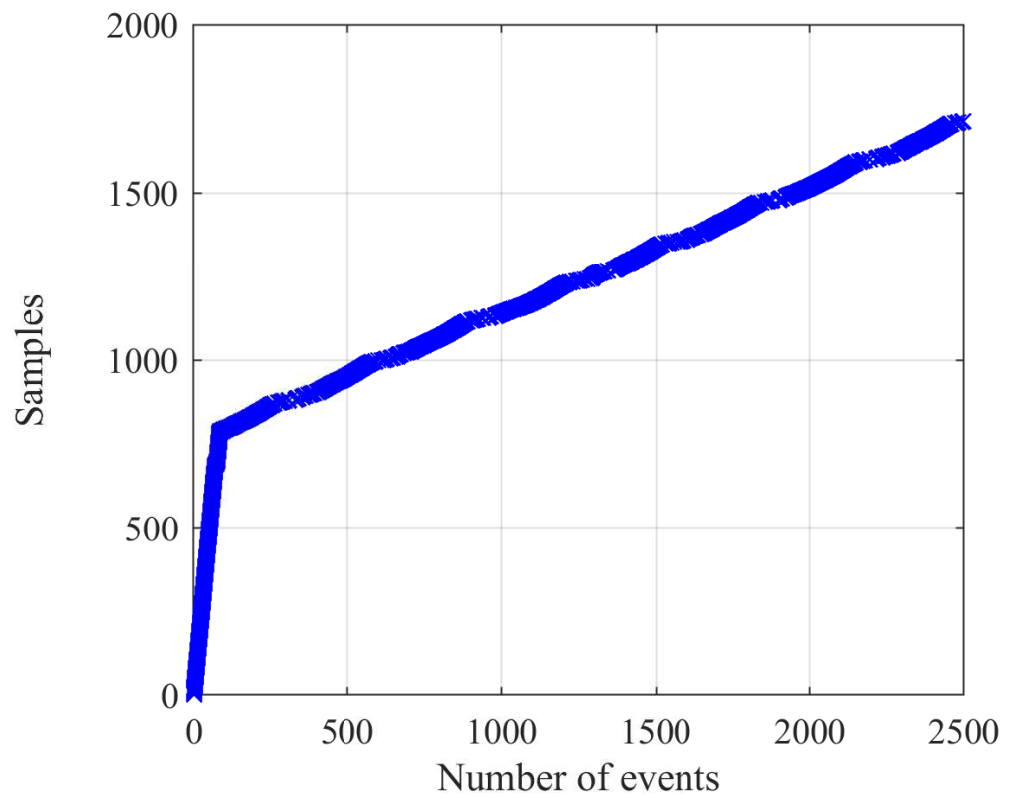


Figure 18. Cumulative number of events.

Based on the above simulation results, it can be observed by the proposed scheme that the tracking objective and the stability can be obtained, and reducing communication burden and meeting preset state limits can also be achieved.

6. Conclusions

An adaptive event-triggered controller approach for state-constrained pure-feedback FONs with input delay, unknown actuator saturation, and external disturbances has been proposed. By employing the BLFs, backstepping technique, and auxiliary compensation system to handle input delay, the constraints are not violated. The fractional-order dynamic surface filters are used to deal with the complexity of the recursive procedure. The ETC strategy is applied to overcome the communication burden from the limited communication resources. The effectiveness can be verified by the simulation results. In the future, the controller design issue for time-delay switching FONs will be considered, and the fractional-order circuit system will be built to verify the effectiveness of the proposed algorithm.

Author Contributions: Methodology, C.W. and M.L.; Software, M.L.; Formal analysis, C.W.; Data curation, J.Y.; Writing—original draft, J.Y.; Visualization, J.Y.; Supervision, C.W.; Project administration, M.L. All authors have read and agreed to the published version of the manuscript.

Funding: This paper was supported by the National Natural Science Foundation of China (62205280).

Data Availability Statement: Data are contained within the article.

Conflicts of Interest: The authors declare no conflict of interest.

Appendix A

Proof of Theorem 1. (1) The proof of Theorem 1-(i): It is true that

$$D^\alpha \zeta_i = D^\alpha a_{i,l} - D^\alpha a_{i-1} = -\frac{\zeta_i}{\kappa_i} + H_i(\cdot), i = 2, 3, \dots, n$$

where

$$H_i(\cdot) = -\sum_{j=1}^i \frac{\partial a_{i-1}}{\partial x_j} D^\alpha x_j - \frac{\partial a_{i-1}}{\partial W_{i-1}} D^\alpha W_{i-1} - \frac{\partial a_{i-1}}{\partial a_{i-1,l}} D^\alpha a_{i-1,l}$$

$$i = 2, 3, \dots, n$$

For constants $\delta_{y_r} > 0$ and $\Theta_\delta > 0$, the set $\Omega_{y_r} = \left\{ (y_r \ D^\alpha y_r \ D^{2\alpha} y_r)^\top \mid y_r^2 + (D^\alpha y_r)^2 + (D^{2\alpha} y_r)^2 \leq \delta_{y_r} \right\}$ and $\Omega_i = \left\{ \frac{1}{2} \sum_{j=1}^i \ln \frac{k_{b_j}^2}{k_{b_j}^2 - \chi_j^2} + \sum_{j=1}^i \frac{1}{2\gamma_j} \tilde{W}_j^\top \tilde{W}_j + \frac{1}{2} \sum_{j=1}^{i-1} \zeta_{j+1}^2 \leq \Theta_\delta \right\}$ are compact. Then, $\Omega_{y_r} \times \Omega_i$ is compact, and there is a $\Xi_j > 0$, s.t. $|H_j| \leq \Xi_j$. Therefore, the following inequality holds:

$$|\zeta_j H_j| \leq \frac{\zeta_j^2 \Xi_j^2}{2q_j} + \frac{q_j}{2}$$

where $q_j > 0$.

Based on error $\tilde{\theta}_i = \theta_i^* - \theta_i$ and $\tilde{\omega}_i = \omega_i^* - \omega_i$, it holds

$$\tilde{\theta}_i \theta_i \leq \frac{1}{2} \theta_i^{*2} - \frac{1}{2} \tilde{\theta}_i^2$$

$$\tilde{\omega}_i \omega_i \leq \frac{1}{2} \omega_i^{*2} - \frac{1}{2} \tilde{\omega}_i^2$$

Then, we can obtain

$$\begin{aligned}
 D^\alpha V_n &\leq - \sum_{i=1}^{n-1} \frac{b_i g_{i \min} \chi_i^2}{k_{b_i}^2 - \chi_i^2} - \frac{h_{\min} b_n \chi_n^2}{k_{b_n}^2 - \chi_n^2} + \sum_{i=1}^{n-1} \frac{\zeta_i^2}{g_{i \min}} \\
 &+ \sum_{i=1}^{n-1} \frac{g_{i \min}}{2\gamma_i} \phi_i \theta_i^{*2} + \frac{h_{\min}}{2\gamma_n} \phi_n \theta_n^{*2} - \sum_{i=1}^{n-1} \frac{g_{i \min}}{2\gamma_i} \phi_i \tilde{\theta}_i^2 \\
 &+ \sum_{i=1}^{n-1} \frac{g_{i \min}}{2\zeta_i} \varphi_i \omega_i^{*2} + \frac{h_{\min}}{2\zeta_n} \varphi_n \omega_n^{*2} - \sum_{i=1}^{n-1} \frac{g_{i \min}}{2\zeta_i} \varphi_i \tilde{\omega}_i^2 \\
 &- \frac{h_{\min}}{2\zeta_n} \varphi_n \tilde{\omega}_n^2 + \sum_{i=2}^n \left(\frac{\delta_{i-1}^2 g_{i-1 \max}^2}{2g_{i-1 \min}} - \frac{1}{\kappa_i} + \frac{\Xi_i^2}{2q_i} \right) \zeta_i^2 \\
 &+ \frac{3\zeta_n^2}{2h_{\min}} + \sum_{i=1}^n \frac{c_i^2}{2} + \sum_{i=2}^n \frac{q_i}{2} + \frac{\delta_{n-1}^2 g_{n-1 \max}^2}{2g_{n-1 \min}} \tilde{u}_s^2 \\
 &- \frac{h_{\min}}{2\gamma_n} \phi_n \tilde{\theta}_n^2 + 0.557\kappa^* \\
 &\leq -\rho V_n + M
 \end{aligned}$$

where

$$\begin{aligned}
 \rho &= \min\{2b_i g_{i \min}, h_{\min} b_n, \phi_i, \varphi_i, E_j, i = 1, \dots, n-1; j = 2, \dots, n\} \\
 M &= \sum_{i=1}^{n-1} \frac{\zeta_i^2}{g_{i \min}} + \frac{3\zeta_n^2}{2h_{\min}} + \sum_{i=1}^n \frac{c_i^2}{2} + \sum_{i=1}^{n-1} \frac{g_{i \min}}{2\zeta_i} \varphi_i \omega_i^{*2} \\
 &+ \sum_{i=1}^{n-1} \left(\frac{g_{i \min}}{2\gamma_i} \phi_i \theta_i^{*2} + \frac{h_{\min}}{2\gamma_n} \phi_n \theta_n^{*2} \right) + \frac{h_{\min}}{2\zeta_n} \varphi_n \omega_n^{*2} \\
 &+ \frac{\delta_{n-1}^2 g_{n-1 \max}^2}{2g_{n-1 \min}} \tilde{u}_s^2 + \sum_{i=2}^n \frac{q_i}{2} + 0.557\kappa^* \\
 E_j &= \frac{\delta_{j-1}^2 g_{j-1 \max}^2}{2g_{j-1 \min}} - \frac{1}{\kappa_j} + \frac{\Xi_j^2}{2q_j}
 \end{aligned}$$

According to Lemma 4, it is easily to obtain

$$V_n(t) \leq V_n(0)E_{(\alpha,1)}(-\rho t^\alpha) + \frac{M\theta}{\rho}$$

Based on Lemma 1, it holds that

$$V_n \leq \frac{M\theta}{\rho}, t \rightarrow \infty \tag{A1}$$

According to the inequality (A1), one can obtain the boundedness of $\ln k_{b_i}^2 / (k_{b_i}^2 - \chi_i^2)$, thus $|\chi_i|$ remains in the set $|\chi_i| < k_{b_i}$. Also, it holds that $\tilde{\theta}_i$, $\tilde{\omega}_i$, and ζ_j are bounded. Since $\tilde{\theta}_i = \theta_i^* - \theta_i$ and $\tilde{\omega}_i = \omega_i^* - \omega_i$, one can obtain that θ_i and ω_i are bounded. Due to χ_1 and $y_r(t)$ are bounded, x_1 is bounded. Due to (14), a_1 is bounded and satisfies $|a_1| < a_{1 \max}, a_{1 \max} > 0$. Using $\chi_2 = x_2 - a_{2,l}$ and $\zeta_2 = a_{2,l} - a_1 < \sqrt{2V_n}$, one can obtain that $a_{2,l}$ and x_2 are bounded. Similarly, based on the boundedness of $u_s(t)$ from (5), the boundedness of states $x_i, i = 3, \dots, n$ and virtual controllers $a_i, i = 2, \dots, n$ are obtained. From (A1), it holds that $\frac{1}{2} \ln k_{b_i}^2 / (k_{b_i}^2 - \chi_i^2) \leq V_n(0)E_{(\alpha,1)}(-\rho t^\alpha) + M\theta/\rho$, which implies that $|\chi_i| \leq k_{b_k} \sqrt{1 - e^{-2V_n(0)E_{(\alpha,1)}(-\rho t^\alpha) - 2M\theta/\rho}}$. That is $\chi_i \in \Omega_\chi, i = 1, 2, \dots, n$.

(2) The proof of Theorem 1-(ii): Based on $x_1 = \chi_1 + y_r(t)$ and $|y_r(t)| \leq A_0$ from Assumption 3, one has $|x_1| \leq |\chi_1| + |y_r(t)| < k_{b_1} + A_0$. Define $k_{b_1} = k_{c_1} - A_0$, one obtain $|x_1| < k_{c_1}$. Due to $x_2 = \chi_2 + \zeta_2 + a_1$ and $|\zeta_2| \leq \sqrt{2(V_n(0)E_{(\alpha,1)}(-\rho t^\alpha) + M\theta/\rho)}^{\frac{1}{2p}} \leq \Delta_2, \Delta_2 > 0$, yielding $|x_2| \leq |\chi_2| + |\zeta_2| + |a_1| < k_{b_2} + \Delta_2 + a_{1 \max}$. Let $k_{b_2} = k_{c_2} -$

$\Delta_2 - a_{1 \max}$, one can obtain $|x_2| < k_{c_2}$. Similarly, one can in turn obtain $|x_i| < k_{c_i}$, $i = 3, \dots, n$.

- (3) The proof of Theorem 1-(iii): From the sampling error $Y(t) = \Theta(t) - v(t)$, one can obtain $D^\alpha |Y(t)| = \text{sign}(Y(t)) D^\alpha Y(t) \leq |D^\alpha \Theta(t)|$. Due to (49), $D^\alpha \Theta(t)$ is bounded, and $\exists \bar{\zeta} > 0$ satisfying $|D^\alpha \Theta(t)| < \bar{\zeta}$. According to $Y(t_k) = 0$ and $\lim_{t \rightarrow t_{k+1}} Y(t) = \lambda_2^*$, one can obtain $t_{k+1} - t_k \geq \lambda_2^* / \bar{\zeta}$, avoiding the Zeno phenomenon.

□

References

- West, B.J.; Bologna, M.; Grigolini, P. *Physics of Fractal Operators*; Springer: Berlin/Heidelberg, Germany, 2003; Volume 10.
- Bagley, R.L.; Torvik, P.J. On the fractional calculus model of viscoelastic behavior. *J. Rheol.* **1986**, *30*, 133–155. [\[CrossRef\]](#)
- Li, Y.; Chen, Y.; Podlubny, I. Mittag-Leffler stability of fractional order nonlinear dynamic systems. *Automatica* **2009**, *45*, 1965–1969. [\[CrossRef\]](#)
- Sun, H.; Zhang, Y.; Baleanu, D.; Chen, W.; Chen, Y. A new collection of real world applications of fractional calculus in science and engineering. *Commun. Nonlinear Sci. Numer. Simul.* **2018**, *64*, 213–231. [\[CrossRef\]](#)
- Soleimanizadeh, A.; Nekoui, M.A. Optimal type-2 fuzzy synchronization of two different fractional-order chaotic systems with variable orders with an application to secure communication. *Soft Comput.* **2021**, *25*, 6415–6426. [\[CrossRef\]](#)
- Li, X.; Mou, J.; Xiong, L.; Wang, Z.; Xu, J. Fractional-order double-ring erbium-doped fiber laser chaotic system and its application on image encryption. *Opt. Laser Technol.* **2021**, *140*, 107074. [\[CrossRef\]](#)
- Shi, J.; He, K.; Fang, H. Chaos, Hopf bifurcation and control of a fractional-order delay financial system. *Math. Comput. Simul.* **2022**, *194*, 348–364. [\[CrossRef\]](#)
- Wang, Y.L.; Jahanshahi, H.; Bekiros, S.; Bezzina, F.; Chu, Y.M.; Aly, A.A. Deep recurrent neural networks with finite-time terminal sliding mode control for a chaotic fractional-order financial system with market confidence. *Chaos Solitons Fractals* **2021**, *146*, 110881. [\[CrossRef\]](#)
- Jin, T.; Xia, H.; Deng, W.; Li, Y.; Chen, H. Uncertain fractional-order multi-objective optimization based on reliability analysis and application to fractional-order circuit with caputo type. *Circuits Syst. Signal Process.* **2021**, *40*, 5955–5982. [\[CrossRef\]](#)
- Mirzajani, S.; Aghababa, M.P.; Heydari, A. Adaptive T-S fuzzy control design for fractional-order systems with parametric uncertainty and input constraint. *Fuzzy Sets Syst.* **2018**, *365*, 22–39. [\[CrossRef\]](#)
- Liu, H.; Li, S.; Wang, H.; Sun, Y. Adaptive fuzzy control for a class of unknown fractional-order neural networks subject to input nonlinearities and dead-zones. *Inf. Sci.* **2018**, *454–455*, 30–45. [\[CrossRef\]](#)
- Song, S.; Park, J.H.; Zhang, B.; Song, X.; Zhang, Z. Adaptive Command Filtered Neuro-Fuzzy Control Design for Fractional-Order Nonlinear Systems With Unknown Control Directions and Input Quantization. *IEEE Trans. Syst. Man Cybern. Syst.* **2020**, *51*, 7238–7249. [\[CrossRef\]](#)
- Hu, T.; He, Z.; Zhang, X.; Zhong, S. Event-triggered consensus strategy for uncertain topological fractional-order multiagent systems based on Takagi–Sugeno fuzzy models. *Inf. Sci.* **2021**, *551*, 304–323. [\[CrossRef\]](#)
- Fei, J.; Wang, H.; Fang, Y. Novel neural network fractional-order sliding-mode control with application to active power filter. *IEEE Trans. Syst. Man Cybern. Syst.* **2021**, *52*, 3508–3518. [\[CrossRef\]](#)
- Cao, B.; Nie, X. Event-triggered adaptive neural networks control for fractional-order nonstrict-feedback nonlinear systems with unmodeled dynamics and input saturation. *Neural Netw.* **2021**, *142*, 288–302. [\[CrossRef\]](#)
- Liu, H.; Pan, Y.; Cao, J.; Wang, H.; Zhou, Y. Adaptive neural network backstepping control of fractional-order nonlinear systems with actuator faults. *IEEE Trans. Neural Netw. Learn. Syst.* **2020**, *31*, 5166–5177. [\[CrossRef\]](#) [\[PubMed\]](#)
- Zhan, Y.; Tong, S. Adaptive fuzzy output-feedback decentralized control for fractional-order nonlinear large-scale systems. *IEEE Trans. Cybern.* **2021**, *52*, 12795–12804. [\[CrossRef\]](#)
- Liu, Y.; Zhang, H.; Shi, Z.; Gao, Z. Neural-Network-Based Finite-Time Bipartite Containment Control for Fractional-Order Multi-Agent Systems. *IEEE Trans. Neural Netw. Learn. Syst.* **2022**, *34*, 7418–7429. [\[CrossRef\]](#)
- Dhanalakshmi, P.; Senpagam, S.; Mohanapriya, R. Finite-time fuzzy reliable controller design for fractional-order tumor system under chemotherapy. *Fuzzy Sets Syst.* **2022**, *432*, 168–181. [\[CrossRef\]](#)
- Wang, C.; Cui, L.; Liang, M.; Li, J.; Wang, Y. Adaptive Neural Network Control for a Class of Fractional-Order Nonstrict-Feedback Nonlinear Systems With Full-State Constraints and Input Saturation. *IEEE Trans. Neural Netw. Learn. Syst.* **2021**, *33*, 6677–6689. [\[CrossRef\]](#)
- Zouari, F.; Ibeas, A.; Boukroune, A.; Cao, J.; Arefi, M.M. Adaptive neural output-feedback control for nonstrict-feedback time-delay fractional-order systems with output constraints and actuator nonlinearities. *Neural Netw.* **2018**, *105*, 256–276. [\[CrossRef\]](#)
- Shahvali, M.; Azarbahram, A.; Naghibi-Sistani, M.B.; Askari, J. Bipartite consensus control for fractional-order nonlinear multi-agent systems: An output constraint approach. *Neurocomputing* **2020**, *397*, 212–223. [\[CrossRef\]](#)

23. Zouari, F.; Ibeas, A.; Boulkroune, A.; Jinde, C.; Arefi, M.M. Neural network controller design for fractional-order systems with input nonlinearities and asymmetric time-varying Pseudo-state constraints. *Chaos Solitons Fractals* **2021**, *144*, 110742. [[CrossRef](#)]
24. Yu, Z.; Zhang, Y.; Jiang, B.; Su, C.Y.; Fu, J.; Jin, Y.; Chai, T. Nussbaum-based finite-time fractional-order backstepping fault-tolerant flight control of fixed-wing UAV against input saturation with hardware-in-the-loop validation. *Mech. Syst. Signal Process.* **2021**, *153*, 107406. [[CrossRef](#)]
25. Alipour, M.; Malekzadeh, M.; Ariaei, A. Active fractional-order sliding mode control of flexible spacecraft under actuators saturation. *J. Sound Vib.* **2022**, *535*, 117110. [[CrossRef](#)]
26. Ju, X.; Wei, C.; Xu, H.; Wang, F. Fractional-order sliding mode control with a predefined-time observer for VTVL reusable launch vehicles under actuator faults and saturation constraints. *ISA Trans.* **2022**, *129*, 55–72. [[CrossRef](#)] [[PubMed](#)]
27. Geng, W.T.; Lin, C.; Chen, B. Observer-based stabilizing control for fractional-order systems with input delay. *ISA Trans.* **2020**, *100*, 103–108. [[CrossRef](#)]
28. Keighobadi, J.; Pahnehkolaei, S.M.A.; Alfi, A.; Machado, J. Command-filtered compound FAT learning control of fractional-order nonlinear systems with input delay and external disturbances. *Nonlinear Dyn.* **2022**, *108*, 293–313. [[CrossRef](#)]
29. Zirkohi, M.M. Robust adaptive backstepping control of uncertain fractional-order nonlinear systems with input time delay. *Math. Comput. Simul.* **2022**, *196*, 251–272. [[CrossRef](#)]
30. Liu, S.; Wang, H.; Li, T. Adaptive composite dynamic surface neural control for nonlinear fractional-order systems subject to delayed input. *ISA Trans.* **2022**, *134*, 122–133. [[CrossRef](#)]
31. Zou, W.; Mao, J.; Xiang, Z. Adaptive Fuzzy Finite-Time Sampled-Data Control for A Class of Fractional-Order Nonlinear Systems. *IEEE Trans. Fuzzy Syst.* **2024**, 1–14. [[CrossRef](#)]
32. Ha, S.; Chen, L.; Liu, D.; Liu, H. Command Filtered Adaptive Fuzzy Control of Fractional-Order Nonlinear Systems with Unknown Dead Zones. *IEEE Trans. Syst. Man Cybern. Syst.* **2024**, 1–12. [[CrossRef](#)]
33. Li, D.; Dong, J. Fractional-Order Systems Optimal Control via Actor-Critic Reinforcement Learning and Its Validation for Chaotic MFET. *IEEE Trans. Autom. Sci. Eng.* **2024**, 1–10. [[CrossRef](#)]
34. Xing, Y.; Wang, Y. Finite-Time Adaptive NN Backstepping Dynamic Surface Control for Input-Delay Fractional-Order Nonlinear Systems. *IEEE Access* **2023**, *11*, 5206–5214. [[CrossRef](#)]
35. Podlubny, I. *Fractional Differential Equations*; Academic Press: Cambridge, MA, USA, 1999; p. 2.
36. Das, S. *Functional Fractional Calculus for System Identification and Controls*; Springer: Berlin/Heidelberg, Germany, 2008.
37. Duarte-Mermoud, M.A.; Aguila-Camacho, N.; Gallegos, J.A.; Castro-Linares, R. Using general quadratic Lyapunov functions to prove Lyapunov uniform stability for fractional order systems. *Commun. Nonlinear Sci. Numer. Simul.* **2015**, *22*, 650–659. [[CrossRef](#)]
38. Aguila Camacho, N.; Duarte Mermoud, M.A.; Gallegos, J.A. Lyapunov functions for fractional order systems. *Commun. Nonlinear Sci. Numer. Simul.* **2014**, *19*, 2951–2957. [[CrossRef](#)]
39. Chen, W.; Dai, H.; Song, Y.; Zhang, Z. Convex Lyapunov functions for stability analysis of fractional order systems. *IET Control Theory Appl.* **2017**, *11*, 1070–1074. [[CrossRef](#)]
40. Gong, P. Distributed tracking of heterogeneous nonlinear fractional-order multi-agent systems with an unknown leader. *J. Frankl.-Inst.-Eng. Appl. Math.* **2017**, *354*, 2226–2244. [[CrossRef](#)]
41. Ren, B.; Ge, S.S.; Tee, K.P.; Lee, T.H. Adaptive Neural Control for Output Feedback Nonlinear Systems Using a Barrier Lyapunov Function. *IEEE Trans. Neural Netw.* **2010**, *21*, 1339–1345.
42. Tee, K.P.; Ge, S.S.; Tay, E.H. Barrier Lyapunov Functions for the control of output-constrained nonlinear systems. *Automatica* **2009**, *45*, 918–927. [[CrossRef](#)]
43. Polycarpou, M.M. Stable adaptive neural control scheme for nonlinear systems. *IEEE Trans. Autom. Control* **1996**, *41*, 447–451. [[CrossRef](#)]
44. Sanner, R.M.; Slotine, J.J. Gaussian networks for direct adaptive control. *IEEE Trans. Neural Netw.* **1992**, *3*, 837–863. [[CrossRef](#)] [[PubMed](#)]
45. Wang, H.; Chen, B.; Liu, X.; Liu, K.; Lin, C. Robust Adaptive Fuzzy Tracking Control for Pure-Feedback Stochastic Nonlinear Systems With Input Constraints. *IEEE Trans. Cybern.* **2013**, *43*, 2093–2104. [[CrossRef](#)] [[PubMed](#)]
46. Yu, J.; Shi, P.; Dong, W.; Lin, C. Command Filtering-Based Fuzzy Control for Nonlinear Systems with Saturation Input. *IEEE Trans. Cybern.* **2017**, *47*, 2472–2479. [[CrossRef](#)] [[PubMed](#)]
47. Shao, S.; Chen, M.; Chen, S.; Wu, Q. Adaptive neural control for an uncertain fractional-order rotational mechanical system using disturbance observer. *IET Control Theory Appl.* **2016**, *10*, 1972–1980. [[CrossRef](#)]
48. Xu, B.; Chen, D.; Zhang, H.; Wang, F. Modeling and stability analysis of a fractional-order Francis hydro-turbine governing system. *Chaos Solitons Fractals* **2015**, *75*, 50–61. [[CrossRef](#)]
49. Ni, J.; Liu, L.; Liu, C.; Hu, X. Fractional order fixed-time nonsingular terminal sliding mode synchronization and control of fractional order chaotic systems. *Nonlinear Dyn.* **2017**, *89*, 2065–2083. [[CrossRef](#)]
50. Petras, I. A note on the fractional-order Chua's system. *Chaos Solitons Fractals* **2008**, *38*, 140–147. [[CrossRef](#)]

51. Wang, M.; Liu, X.; Shi, P. Adaptive Neural Control of Pure-Feedback Nonlinear Time-Delay Systems via Dynamic Surface Technique. *IEEE Trans. Syst. Man Cybern. Part B* **2011**, *41*, 1681–1692. [[CrossRef](#)]
52. Jafari, A.A.; Mohammadi, S.M.A.; Naseriyeh, M.H. Adaptive type-2 fuzzy backstepping control of uncertain fractional-order nonlinear systems with unknown dead-zone. *Appl. Math. Model.* **2019**, *69*, 506–532. [[CrossRef](#)]

Disclaimer/Publisher’s Note: The statements, opinions and data contained in all publications are solely those of the individual author(s) and contributor(s) and not of MDPI and/or the editor(s). MDPI and/or the editor(s) disclaim responsibility for any injury to people or property resulting from any ideas, methods, instructions or products referred to in the content.